Javier Almendros (Referee #1)

We thank the reviewer for the appreciation of our work and the very helpful, careful and detailed review.

Reviewer 1: GENERAL COMMENTS

This is an interesting paper dealing with the application of array techniques to the problem of earthquake location. It constitutes a very clear demonstration of the fact that when a distributed network around the seismogenic area is not available, seismic arrays are a feasible alternative. The authors deal with earthquakes that are distributed around Fogo and Brava islands. Any seismic network based on land stations will be ill-suited, due to the limited extent of the Cape Verde islands. The authors use time-domain beam-forming at three seismic arrays to estimate the back-azimuths to the source, and design a scheme based on probabilities to pinpoint the epicenter locations.

However, there are some aspects of the work that need a critical revision. I address some of them below.

EPICENTRAL LOCATION

The locations obtained by the multi-array approach are limited to the determination of the epicenters using the estimates of back-azimuth. But sometimes the authors seem to oversee this limitation. At several points in the paper (see detailed comments below) you seem to imply that your method is better that others because you do not need a velocity model, with all the uncertainties that it brings to the calculations. However this is not a real advantage, since you provide only epicentral locations. The determination of depth requires some knowledge or assumptions about the velocity structure.

There is some discussion about source depths, although they are heterogeneous and somewhat confusing. In general, depth estimates are not addressed systematically. Sometimes a velocity model is assumed, either a two-layer model (line 229) or the model of Vales et al. 2014 (line 203) which is more complex. At one instance the depth is fixed (line 230). Depths are obliterated at the beginning but they are brought back during the discussion. I suggest that, if possible, you should exploit fully the information provided by the arrays, not only the back-azimuths but also the apparent slowness results, and include depths as part of the results. Of course the depths would be biased by the choice of velocity model, but at least you would have an estimate.

Answer: It is true, that the method we chose only reveals epicentral locations. This may seem like a disadvantage, but it provides the possibility to determine the epicentral location without any a priori knowledge about the velocity structure. In the case of Fogo and Brava, we decided not to rely on the velocity model, as the available models either provide an average structure for the whole Cape Verde archipelago or of other islands with older structures than Fogo and Brava.
Nevertheless, we agree with the reviewer, that we need to point out more strongly, that we only determine epicentral locations. We modified this in the revised manuscript.
Changes in manuscript: lines 13, 52, 91, 113, 142-143, 201, 240, 317, 342, 344.

R1: EARTHQUAKES VS HYBRIDS

The classification of seismic signals in "earthquakes" and "hybrid events" is not clear. Figure 7 compares the seismogram and spectrogram of a volcano-tectonic earthquake and a hybrid event, both recorded at the AF array on Fogo. Why don't you think that the hybrid event is in reality a small volcano-tectonic earthquake located in Fogo? I don't see a low-frequency coda, or any hint of a band-limited frequency content. Looking at the spectrum, it is true that there is relatively more energy in the 0-10 Hz band. For the hybrid, the peaks in the 0-10 and 10-20 Hz bands have similar heights.

While for the VT earthquake there is definitely more energy in the 10-20 Hz band. Still, this could be an effect of lower signal-to-noise ratio. The noise seems to have bursts of energy in the 0-10 Hz band (before, during and after the event), so the difference could be just an effect of the size of the earthquake.
Figure S2 shows a single volcano-tectonic earthquake recorded at the AF array on Fogo and the BR array on Brava. The right plot looks similar to Figure 7b, except for the difference in signal-to-noise ratio.
In any case, I suggest that you justify your classification, showing hybrid events that look clearly different from local earthquakes. This has no impact in the method that you are presenting, which is valid for any earthquake: volcano-tectonic, hybrid, or whatever. But it is important for the interpretation of the activity in the discussion.

A.: In contrast to a volcano-tectonic earthquake, a hybrid event shows a smooth transition from higher to lower frequencies. In the case of a hybrid event there is no S-phase identifiable and in the coda (for about 15 to 20 seconds) there is still more energy available in the 0-10 Hz band than before the event event (and in comparison with a VT earthquake). In contrast, even for the small VT earthquakes on Fogo two phases are detectable. To make this point clearer, we replaced the example earthquake displayed in Figure 8a (formerly 7a) with an earthquake from Fogo. By this, the difference between the event types should become clearer. Additionally, we added a figure to the supplementary material which shows the spectrogram of all components of a hybrid event. In this figure the low frequency content of the coda becomes evident.
With our discrimination between volcano-tectonic earthquakes and hybrid events we also follow earlier studies on the seismicity of Fogo (e.g. Faria and Fonseca, 2014).
We do not exclude that an earthquake might be involved in the triggering of the hybrid events. McNutt (2000) refers to a mechanism, where an earthquake sets an adjacent fluid-filled cavity into oscillation. This could explain the high-frequency content in the beginning of the signal and the lower frequencies in the coda. Nevertheless, there are also other hypotheses of possible mechanisms for hybrid events, which are also capable to explain their occurrence on Fogo (see discussion in the text).
Changes: lines 237-238, Fig. 8, Fig. S9.

R1: ARRAY ABERRATIONS

I don't agree on the use of the term "aberration" referred to the array, e.g. line 64: "seismic arrays can exhibit systematic aberrations of backazimuth and slowness", line 186: "Effects along the ray path from the source to the array, such as heterogeneities, can result in a systematic aberration of the array".

The heterogeneity of the medium can have an effect on wave propagation, resulting in rays impinging at the array site with back-azimuths that do not point to the source. See for example the interesting results of Garcia-Yeguas et al. GJI 2011. However, this cannot be pinned to the array! The seismic arrays are working ok, providing the directions with which the wavefronts are propagating through the array, these estimates are not biased in any way. The wavefield distortions (or aberrations) are produced in the medium. Therefore, I'd rather talk about ray bending or back-azimuth deviations, instead of array aberrations.

A.: Thank you for pointing this out. We changed the terming accordingly.
Changes: lines 18-19, 62-63, 149-150, 162, 176, 193-194, 319, 323-324, 346-347.

R1: METHOD

The description of the method, and particularly the uncertainty estimates, is a bit confusing. You take as uncertainty the standard deviation of the maximum energy obtained by varying the start and duration of the stacking window. How do you obtain the standard deviation of back-azimuth and apparent slowness? Are these the values reported in tables S1,S2? Standard deviations of back-azimuth in those tables are large

(around 100 degrees), but in the figures the beams seem to be much narrower. The width of the back-azimuth wedges is related to the uncertainty of the solutions, but I don't fully understand this relationship.

A.: Yes, the standard deviation values are reported in the tables S1 and S2. Regarding for example Figure 4 (formerly 6), the beam of array AF (southern beam at Fogo) exhibits a standard deviation of 73°. This corresponds to an error of 20%. The beam width thus corresponds to 80% of the maximum energy of the "original" beam determined during the array analysis (i.e. the beam resulting from the manually chosen stacking window). In this way, the backazimuth wedges are related to the width of the "original" beam. This beam is not necessarily symmetric and the choice of the errors taken from the standard deviation of the backazimuth allows us to include possible asymmetries of the beam. Additionally, in this way also sidelobes are included in the multi-array analysis. This can be seen in Fig. 4 (formerly 6), where a small beam at array CG (western array on Fogo) points to the south-southwest.

However, we clarified this in the revised manuscript.
Changes: lines 127-137.

R1: Additionally, the width of the array response is not considered at all. Even if the energy stack in figure 3 provides a very narrow peak, you should consider the uncertainty produced by the finite array response. In figure S1 I see that the central peak has a diameter of about 0.1 s/km, this should be always added to any uncertainty estimate.

A.: One advantage of the choice of a time-domain array analysis is the implicit inclusion of a broad frequency band in the analysis. The conventional array response is only estimated for a single frequency. Correspondingly, the stacking of (integration over) the array responses for a wide frequency band would also lead to a much narrower peak. We added this information to the supplement.
Changes: Figure caption of Fig. S1.

R1: For earthquakes, apparent slowness is smaller at BR. This should imply a larger uncertainty in back-azimuth, which is not clear in the plots.

A.: Yes, this is true, BR shows typically large uncertainties in the backazimuth. Therefore, in many cases it shows the highest values for the standard deviation of the BAZ. However, the higher uncertainties also cause many energy contour plots (used for the BAZ estimations) of the array BR to be rejected, as the results are unstable. For example, if a small variation in the choice of the stacking window or different frequency bands lead to a strong variation of the beam, this result is considered unstable and thus rejected.

R1: Why do you use the time-domain beam-forming method? There are other options that may provide improved estimates of the back-azimuth and apparent slowness. Have you tested any other array method?

A.: We have also tested an f-k analysis (software of NORSAR). However, we think that the implicit inclusion of a broad frequency band, which leads to a strongly narrowed energy peak, and the narrow stacking window around one particular phase at the reference station provide strong advantages compared to the conventional f-k analysis. As described in the text, time-domain analysis has additional benefits with regards to the phase of interest.
The implicit inclusion of a wide frequency band in the time-domain analysis not only reduces the amount of possible sidelobes, but also allows for the analysis of events with different frequency content.

R1: How are the results from the three arrays combined to provide the locations? (as in figure 6). It looks like you simply add the "energy" grids obtained for the arrays. However, if you interpret these maps in terms of probabilities of a grid node being the epicenter location, it make more sense multiplying them. After all this is an "and" operation, you want to determine if the position of a given node complies with the back-azimuths at array AF AND array CG AND array BR.

A.: We do not interpret the maps in terms of probabilities of a grid node. But instead we use the sum of the normalized energy distribution derived from the single arrays. We found this method to give the best results in comparison to the conventional network localization.

R1: NETWORK LOCATIONS

I'd like to have some information about the quality of the network locations. They are used as ground truth in the comparison with the array locations. But the station coverage is poor and I assume that the network locations may have large uncertainties as well, even if you restrict them to the best cases. Perhaps you can show examples with error ellipses (in the supplementary information?).

A.: This is a good point; we added a map to the supplementary material that shows the locations of the (classical) network-based analysis.
Changes: lines 170-171, Fig. S5.

R1: OTHER COMMENTS

- line 54: the method of localization "has the advantage of being independent of velocity models". This is a bit misleading because you are just providing an epicentral location. If you try to locate the earthquake (including depth) you do need a velocity model.

A.: Thank you for pointing this out. In the revised manuscript we emphasized the determination of the epicentral location.
Changes: lines 13, 52, 91, 113, 142-143, 201, 240, 317, 342, 344.

R1: - line 55: "The velocity structure is often very complex in a volcanic regime", I think that the term "regime" is not adequate here. Perhaps "environment", "setting", or "medium". (The same in line 242).

A.: In the revised manuscript we replaced the term "regime" by "environment".
Changes: lines 54, 254, 343.

R1: - lines 57-62: this description of the method is too detailed for the introduction, it could be later in the method section.

A.: We shortened this appropriately.
Changes: lines 57-59.

R1: - section 2, the arrays are made of different types of seismic stations, short period and broadband. I assume you have taken good care of this and removed the instrument response, in order to make the waveforms comparable?

A.: We remove the instrument response during the magnitude determination. However, during the array analysis we apply appropriate filter functions.

R1: - line 73: "the arrays were designed for events with frequencies between 5 and 10 Hz". What do you mean? More than frequency of events, what's important in array design is the wavenumber, that includes the effect of frequency and apparent slowness.

A.: Thank you for pointing this out. We decided to use the array transfer function in terms of frequency and slowness components s_x and s_y (instead of wavenumber). Both formulations are equivalent.
The arrays were designed based on the array transfer function for frequencies between 5 and 10 Hz. We clarified this in the revised manuscript and changed the wording.
Changes: lines 72-73.

R1: - line 83: "absolute slowness", what do you mean with "absolute"?

A.: This term refers to the estimation of the slowness via $s = \sqrt{s_x^2 + s_y^2}$. However, to make this clear, we will replace the term "absolute slowness" with "magnitude of horizontal slowness".
Changes: line 83.

R1: - figures 3,4,5: one figure for one array may be enough to show how the method works.

A.: We decided to show all three figures, as their results are combined in Figure 4 (formerly 6). However, we moved Figures S2.1 and S2.2 (formerly 4 and 5) to the supplementary material.

R1: - line 103: grid size of 124x124. If the grid search extends from -0.3 to 0.3 s/km, the grid spacing is about 0.005 s/km. This is unnecessarily small, given the shape of the array response.

A.: The array response function is only estimated for one particular frequency. However, the time-domain array analysis implicitly includes a broad frequency band, which narrows the central peak and reduces sidelobes.
Additionally, we performed tests with a grid size of 62x62. This would reduce the computation time. However, it turned out, that the results of the analysis with the finer grid were better.

R1: - line 104: "the resulting energy stack is shown in Fig 3b". What do you mean by "energy stack"? You delay and sum the signals in the time domain, thus obtaining a seismogram representing the beam for a given apparent slowness and back-azimuth (e.g. green line in figure 3c). But this is still a time series, how do you get a unique value to be plotted in figure 3b? Is this the maximum amplitude of the beam? Is it the rms?

A.: This is the contour plot of the energy, representing the absolute amplitude of the sum trace for each grid node. We replaced the term "energy stack" by "contour plot of the energy" in the revised manuscript, which should clarify this point.
Changes: line 104.

R1: - line 106: the formula BAZ=90-atan(sx/sy) does not follow the usual convention that BAZ=0 for north direction. When sx=0 we obtain BAZ=90. This formula should be corrected, or else explain your convention for azimuths.

A.: Thank you for pointing this out. Accidentally, the given formula is related with the MATLAB coding that we used. We replaced this with the correct formula $BAZ = \frac{180^\circ}{\pi} atan(\frac{s_x}{s_y})$.
Changes: line 106.

R1: - line 109: "the slowness is related to the angle of incidence by sin(i)=s*vc, with the mean crustal velocity vc". I have two criticisms. First, this s in the formula is APPARENT slowness (or ray parameter). Slowness (without "apparent") is just the inverse of velocity, and therefore it is not related to the incidence angle. Second, this formula is valid at points along the seismic ray, with local values of i, s_ap, and velocity.

I don't think that the use of a "mean crustal velocity" is adequate in this context. What are i and s_ap then? If you are thinking of the arrival at the array, i is the incidence angle at the surface, and s_ap the apparent slowness measured by the array. But then v should be the velocity of the shallow layer, not an average of the crust.

A.: Regarding the first point: In the revised manuscript we adjusted this by using the term "horizontal slowness" or "ray parameter". We prefer to use the terms "horizontal slowness (ray parameter)" as the term apparent is usually used in relation to the velocity.
Regarding the second point: Thank you for pointing this out. We rephrased this by using the term "velocity of the upper layer beneath the array".
Changes: lines 109-110, 326-327.

R1: - figure 6: there is a light-blue beam going SSW from the CG array, what is it? (the same happens in figures 12 and 13). The error bars seem underestimated. In the color scale of this plot, 90% of the maximum seems to correspond to the transition from yellow to orange. But in the map, the error bars do not include that transition, I'd say that the error area should include the whole yellow patch, e.g. +-0.03 degrees approx from the epicenter.

A.: The light-blue (small) beam pointing to the south-southwest from array CG in Fig. 4 (formerly 6) is an example of a sidelobe, which shows an energy corresponding to the standard deviation of the backazimuth. We added this information in the captions.

Unfortunately, a mistake occurred during the estimation of the error. In the revised manuscript we corrected for this mistake. The error bars are indeed far larger than displayed in the original figure. Thanks for bringing this to our attention.

Changes: lines 495-497 (figure caption Fig. 4), Fig. 4.

R1: - figure 6, caption: "the location of maximum energy estimated" is unclear. You are locating the epicenter of an earthquake. The colors indicate the directions in which the beamforming provides maximum energy, but in what sense the overlapping area has more energy? Also the sentence "The beams correspond to the beams" should be rephrased.

A.: We rephrased the figure caption in the revised version of the manuscript.
Changes: lines 494-495 (figure caption Fig. 4).

R1: - line 156: "discrepancy of the amount of detected and with the multi-array analysis located earthquakes", weird sentence, rephrase?

A.: We rephrased this in the revised manuscript.
Changes: line 215.

R1: - line 164: "on Brava the dominant frequencies of the same event are lower", why do you mention this, and even show figure S2? Since the earthquakes are closer to Brava than Fogo, is this an indication of a site effect?

A.: In the discussion we go into more detail on this point (lines 248-256). This is the reason why it is also mentioned in the description of the observations.

R1: - line 166: "ray turning point", that is true for rays propagating downward from the source. For an upward propagating ray there is no turning point.

A.: Thank you for pointing this out. Indeed, this estimate can only be performed for the earthquake signals recorded on Fogo and originating around Brava. This larger distance

ensures that the recorded wavefront propagated downwards from the source. However, we clarified this in the revised manuscript.
Changes: lines 224-226.

R1: - line 180: you superimpose the beams for all hybrids, why would you do that? Are the beams weighted in some way? Why didn't you do this for earthquakes as well? The white boundary in figure 10b leaves out the largest hybrid events, e.g. the northernmost, magnitude 1.5 event. Do you assume that the sources must be the same? What is the interpretation of this figure 10b?

A.: From our analysis it becomes clear that the hybrid events only occur in a certain area on Fogo. The superposition of the beams of the hybrid events gives an idea of the area with the highest probability of occurrence of these events. Under consideration of the uncertainties of the events (errors and possible BAZ deviations), they could possibly share the same source region. The 80% contour line (white line) leaves out the strongest event. However, its error bars are rather large. Therefore, it is not unlikely, that it could be located closer to or within the area of 80% probability of the occurrence of hybrid events.
This approach works well for hybrid events, which are confined to a smaller area than the earthquakes. Additionally, it is known that the earthquakes around Brava frequently change their location. Therefore, such an approach is not useful for the earthquakes we located.

R1: - figure 8: the cumulative number of hybrids seems unrelated to the daily number of hybrids. The curve grows when there are no events (e.g. during April or June 2017), and the peak with 5 events in a day is not coincident with any increase in slope. I think this may be due to building this curve just joining points, when it should have a stair-like aspect (you should have right angles instead of the diagonal). The difference is not significant when there are many earthquakes, as if figure 8a. But it pops out when the number of earthquakes is small, as in figure 8b.

A.: Thank you for pointing this out, we modified the figure accordingly.
Changes: Fig. 9.

R1: - figure 9: very small events (M~0-0.5) near array AF and in areas near Brava, how can you locate these? Do you get good results for these earthquakes even at distances of 30 km from the array? This could be very interesting and emphasize the power of seismic arrays, but of course you need very fine noise conditions to perform the analysis, specially since beam-forming is carried out in the time domain.

A.: Indeed, the noise conditions are the reason, why many of the events with magnitudes below 0.5 are located by using only two arrays. In these cases, the noise condition of the third array typically are too poor. Additionally, they have in common that they occur at nighttime, where man-made noise typically is very low. Regarding the traces, it would indeed be difficult to pick the P-phase at all stations reliably. However, their combination during the beamforming results in a clear P-phase onset of the sum trace. The application of the time-domain analysis is helpful in such a case, as the frequency band of the analysis can be chosen favorably in order to increase the SNR.
We included this point in the discussion of the revised manuscript.
Changes: lines 248-252.

R1: - figure 10 has error bars in the locations of the hybrid events, but there were no error bars in figure 9.

A.: The reason for leaving out the error bars in Figure 10 (formerly 9), is that the number of events is larger than in Figure 11 (formerly 10), which strongly reduces the clarity of the map. However, this is a good point and we added a map to the supplementary material showing the error bars of the earthquakes.

Changes: line 231, Fig. S7.

R1: - section 4.3 is partly related to the method, in fact you refer here to section 3.2. Wouldn't the part on array parameters fit better in the method section?

A.: We agree that there is a relation to the method section. However, we first decided to include this part in the results section, as we present the outcome of different tests of the method based on recorded events. Nevertheless, we moved this section to the method section.
Changes: lines 145-205.

R1: - around line 195: it is not clear if you are talking about the start of the stacking window or the length of the stacking window.

A.: We refer to the start time of the window and the end time.
Changes: line 151.

R1: - line 206: rms < 0.25 s?

A.: Yes, this is the rms of travel time residuals. We added the unit.
Changes: line 169.

R1: - line 207: "(theoretical) back-azimuth". I don't think you should call "theoretical" to the back-azimuth obtained from the network location. The network location constitutes just another estimate of the epicenter location. And given the sparse network distribution, there is no reason to think that the network location will be better than the array location. So I would pick another word, perhaps "reference" back-azimuth?

A.: Thank you for pointing this out. We replaced the term "theoretical" by "reference".
Changes: line 171.

R1: - line 207: "slowness values", you mean apparent slowness? For this you do need a velocity model, I assume you use the same velocity model from Vales et al. (2014) ?

A.: Yes, as for the localization with the classical localization method we also use the velocity model of Vales et al. (2014) for the estimation of the magnitude of horizontal slowness (ray parameter). We included this information (magnitude of horizontal slowness; velocity model) in the revised manuscript.
Changes: line 172.

R1: - figure 11: this is difficult to understand, since you represent back-azimuth and apparent slowness independently. The red dots are located in the coordinates (baz1,s1) given by the array analysis. But the green dots are not located at the coordinates (baz2,s2) given by the network locations. Instead, they are located at (baz2,s1) in the left panels and (baz1,s2) in the right panels. Why splitting them like this? These green points do not represent real estimates, and I find this figure very confusing, I don't know what you want to emphasize with this kind of plot. Have you considered x,y plots instead of polar plots?
- line 211: "yields back-azimuths pointing too far to the south by about 7 degrees", this is difficult to see in figure 11 because all points overlap in a tight cluster.

A.: We have chosen this type of plot because it is actually easier to read than the plot showing the vectors from (baz1,s1) to (baz2, s2).
We do not use x,y plots as especially for the baz components it is easier to see the deviation in a polar plot. Nevertheless, we modified the figure to make the deviations more obvious.
Changes: lines 173-174, Fig. 5.

R1: - figure 12: these examples may serve as a test to understand if your selection of uncertainty levels is adequate. Ideally, the uncertainty region in panels a and c should contain the solution shown in panels b and d. For example, if you choose a level of 0.7 to define the uncertainty region, the solution of panel b would be contained within the uncertainty region of panel a. It is important to understand that even if you use the maximum as best solution (red dots) the source could be anywhere within the uncertainty region (e.g. the orange-yellow areas, sum of energy above 0.7).

A.: This is an interesting point. In fact, the yellow area in e.g. Fig. 6 (formerly 12a) would extend even further to the west if we would choose a map section with limits further to the west. Therefore, the question arises whether the result can be used at all. If the uncertainty becomes too large, the result is not reliable and is discarded. These examples (Fig. 6 (formerly 12 a,c)) are not appropriate to check the level of uncertainty as we would not consider these cases any further for the event localization.

R1: - line 249: "cannot establish a link between them". I agree, I think that even bringing up the subject is a bit far-reached.

A.: It is true, that it is hard to establish a link between them. However, volcano-tectonic earthquakes are rare on Fogo and therefore it is worth noting that they occur in the same area as the deep earthquakes. Due to the difficulty to establish a link between these events, we deliberately kept this point rather short.

R1: - line 260: "from February to March and from June to September". Looking at figure S6 I see that there were more than 10 events in June and from September to November. There is a minimum in August. This does not correspond with your description, there is no increment in the hybrids in the period "June to September".

A.: Yes, indeed, this should read "from September to November". Thank you for pointing this out. We corrected this.
Changes: line 272.

R1: - line 266: "With the multi-array analysis it is not possible to estimate the depth of the events". This is not true in general. You can estimate the depth as well, if you exploit the information from apparent slowness and not only back-azimuth, as demonstrated for example by Almendros et al. 2001 and La Rocca et al. 2004. If you want to keep this sentence, you should specify that you are referring to your own implementation of multiarray analysis, focused on epicenter location.

A.: Thank you for pointing this out. We clarified the statement, that the multi-array method we apply is not suited to estimate the event depth as we do not include a velocity model in our analysis.
Changes: lines 278-279.

R1: - line 281: "Low rupture velocities and strong path effects result in the long low-frequency coda", regarding this discussion see also the paper by Bean et al. 2014 in Nature Geoscience, who discuss the same issue for long-period events.

A.: Thank you for pointing out this interesting reference. We included it in the discussion.
Changes: lines 294-296.

R1: - line 283: "we conclude". It is not clear to me the reason of this whole discussion about the origin of hybrids. It is not based on your results, and I don't see what is the consequence regarding the array analysis. Perhaps you could explain a little more, is there any evidence in the locations, or the array results, pointing to a fluid-related origin? Is there any evidence pointing to the contrary?

A.: "Conclude" may be a bit strong, but we think that this discussion is important. In the revised manuscript we rephrased this sentence.
Changes: lines 297-300.

R1: - line 288: "partly strong", what do you mean?

A.: We removed the term "partly strong".
Changes: line 303.

R1: - line 289: "slowness variations", compared to what?

A.: Slowness variations compared to a simple homogeneous velocity structure as also mentioned in the text.

R1: - line 302: "Being independent of any velocity model and able to locate events", as commented somewhere above, this is misleading. The multi-array method proposed does not use a velocity model BUT is able to identify just epicenters. You should make this clear at all instances, claiming otherwise is misleading. The location of seismic events (hipocentral location, complete with depth) requires a velocity model.

A.: We specified this at the relevant instances by adding the information that we determine the epicentral location of the events.
Changes: lines 13, 52, 91, 113, 142-143, 201, 240, 317, 342, 344.

R1: - line 313: parallel beams imply over-estimated distance? What do you mean exactly? To determine if the distance is over-estimated, you must know the distance. And this is precisely what you are trying to estimate.

A.: Figure 6 (formerly 12) shows what is meant by "over-estimated distance". In view of these observations we included a simple epicentral distance estimation based on S-P travel-time difference estimations (Figure 7 (formerly 13)) to give additional information to the analyst. This is explained further above (lines 188-203). However, we clarified this in the text.
Changes: lines 328-329.

R1: - line 314: "closer to the expected location". What is the expected location?

A.: See above. However, we added a link to Fig. 7 (formerly 13) at this point.
Changes: line 333.

R1: - line 326: "This application allows the event localization without assuming a velocity model". Again, this is misleading. In reality you should talk about epicentral location. You cannot fix the depth without a velocity model.

A.: We clarified this during revision.
Changes: line 342.

R1: - line 341: hybrids show significantly larger apparent velocities than volcano-tectonic earthquakes? You said that in average, at the Fogo arrays the apparent velocity is 7.1 km/s for volcano-tectonic earthquakes from Brava (line 165), and 7.8-8.4 km/s for hybrids (line 178). I don't think this is "significantly larger", specially considering the uncertainties in these estimates.

A.: We rephrased this in the revised manuscript.
Changes: line 358.

R1: - line 348: the mention of volcanic tremor in the conclusions of the paper is out of place.

A.: This information is thought as an outlook and to provide motivation for further analyses of the data.

Referee #2

We thank the reviewer for the careful review and comments and for appreciating our efforts.

Reviewer 2: The manuscript presents an interesting study to locate earthquakes using a number of arrays. Potentially it is a good manuscript for the journal.I However, before this I have several comments and concerns that I think will have to be addressed. Especially I have the feeling there are two different ideas here. I am not sure the multi-array analysis is the important part? Or is it? The discussion seems to focus on the events rather than the method. Maybe that makes the manuscript somewhat difficult to read?
The first main point I have is that the manuscript is fairly difficult to read because of the organisation of the text. For example the introduction talks about the methods and results in far too much detail without the necessary background that then comes in the chapters afterwards (but a bit more introduction and references would be useful in the introduction).

A.: This manuscript presents a relatively new method (use of multi-array and time-domain array analysis) applied to volcanic seismic signals on Fogo and Brava. Therefore, it contains a more detailed description of the method and a discussion of the events analyzed.
We rephrased the introduction slightly. However, we focus on previous studies using multi-array analysis at volcanoes and on previous observations in our study area.
Changes in manuscript: lines 52, 54, 57-59, 62-63, 64.

R2: In chapter 3.2 the first sentence has nothing to do with the rest of the paragraph, while the remaining paragraph seems to fit better in chapter 3.1. Part of 4.1 should be in methods (it discusses errors of the analysis and should be with methods..). The part on error estimation should follow directly from the methods for better flow before then talking about the locations and the discussion, which focusses on the events rather than the method. Please re-write. Also the discussion introduces new results, so these should be in the results section?

This whole organisation makes the reading hard work. Re-writing would clear up much of this difficulty. Indeed the writing in many places could be much more concise there is often unnecessary detail and repetitions.

A.: The first two sentences of section 3.2 introduce the multi-array analysis. This is essential and all following descriptions are based on that idea. This is what follows after the beamforming, which is performed for each array individually. The section 3.2 contains the information on how the results of the beamforming of each array are combined to a multi-array solution.

However, we agree that the structure can be improved and we revised the manuscript and moved section 4.3 to the method section 3.
Changes: lines 145-205.

R2: Using beamforming, information on the velocity is needed, I am not sure how the authors can say that there is no need for knowledge of a velocity model? Have they tried to run the analysis with a non-fitting velocity model? I assume this would greatly worsen the resolution? This should be shown… (it comes back in line 90, so please comment on the size of these uncertainties and what it means to the location errors.)

A.: In array seismology, during the beamforming, no information about the underlying velocity structure is needed. The method is based on the idea, that a plane wave travels across the array. By shifting the traces and summing them up, the direction and the magnitude of slowness of the wavefront are determined (lines 82-86). For details see Rost and Thomas (2002) and Schweitzer et al. (2012), as also cited in the text. As the beamforming does not rely on a velocity model, the combination of the beams allows us to determine the epicenter of the earthquake from the intersecting beams alone, without knowledge about the velocity structure.

R2: Has stacking been done using a plane wavefront or a circular one? Is the wavefront already plane in this distance? Has this been tested?

A.: This is a good point, we assume a plane wavefront. This approximation is in accordance with conditions given in Schweitzer et al. (2012). We estimated that for distances of more than 6 km the plane wave approximation holds. This is the case for the majority of events we analyzed. However, for the few events being located closer to one of the three arrays, the magnitude of slowness becomes small at this particular array and the backazimuth shows a broad uncertainty due to the broadening of the beam. This uncertainty is accounted for during the localization with the multi-array method.

R2: Has the stacking been done with one backazimuth? How different is the backazimuth for each station? This should be shown.

A.: The stacking is done for a complete range of backazimuths by a grid search over the range of horizontal slowness components. Therefore, it is not determined per station but for the whole array.

R2: How much does out-of-plane travelling influence the results? In the presence of strong velocity changes (as possible in volcanic environments), the waves will not travel on the great circle path. Has this influence been tested? This is different from mislocation vectors as discussed later.

A.: If the velocity changes are strong enough to impact the propagation of the wave, this should also lead to errors in a classical localization method. We constrain the possible errors by comparison with the network localization.

R2: The discussion seems to be disconnected from the rest of the manuscript? Where do all the results come from? They were not shown in results? This needs to be better organized as well. Please re-write

A.: The approximations described in the discussion section serve as additional information on the interpretation of the events analyzed. However, these estimations are only rough approximations (e.g. the estimation of the ray path of hybrid events to estimate the depth) and are often too simple to give a reliable result (for example the depth estimation of the hybrid events results in too large depths, which are in contrast to the observations pointing to a shallow source region). Therefore, such approximations should not be shown in the result section, as this may give the impression that these results are considered reliable. We therefore think that these approximations are best discussed in the discussion section.

R2: What are the systematic aberrations? Is this a mislocation vector? This needs a reference! - ah pages later I find that it is indeed the mislocation vector as given by Krüger and Weber. Please move this part of the manuscript when first discussion aberrations. It is out of place that far back.

A.: Thank you for pointing this out, we added a reference at the corresponding position in the text.
Changes: line 64.

R2: Has for the estimation of the mislocation vectors in part 4.3 the topography been taken into account? I assume that the stations are located at different heights? Jacobeit et al., 2013 show that topography has a large influence on the mislocation, not only heterogeneity…

A.: It is true, that the station elevation difference can have a strong influence on the result of the array analysis. Therefore, we carefully tested possible influences under the assumption of the different station elevations according to Schweitzer et al. (2012). It turned out that the station elevation differences are small enough to be neglected.
We added this information to the text.
Changes: lines 180-182.

R2: Is the criterion of 10 times wavelength (line 86) given in this case?

A.: Yes, see above.

R2: How does the chosen filter (which? Please state per event?) influence the resolution?

A.: The influence of the filter has been tested carefully (lines 153-160; Figure S4). It turned out, that the influence of the choice of the cut-off frequencies is very small and entirely covered by the error of the standard deviation of the backazimuth. Therefore, the contribution of the choice of the filter may be neglected.

R2: I am missing a table with station information? Please add to Supp. Mat.

A.: As described in the data availability section, the data including all station locations are available for download at GEOFON (https://geofon.gfz-potsdam.de; https://doi.org/10.14470/4W7562667842).

R2: Where are the locations of all events (2709, line 154) comes from? Have they been located before? By whom? or from catalogue? And how much better is this multiple array beaming? Why can only be 112 of 2709 events be located with the new method? How much better do the locations become when using multi-array methods? This could be part of the discussion

A.: There seems to be a misunderstanding. The 2709 is the total number of events, which we recorded with our network on Fogo and Brava (line 213). Out of these 2709 earthquakes, we located 112 by applying the multi-array analysis. The first reason for this discrepancy is that most earthquakes are of relatively small magnitude and they occur close to (or beneath) Brava. If they are too small, they are covered by noise at the stations on Fogo. As we operate only one array on Brava, this precludes the usage of multiple arrays. The next reason for this discrepancy are the requirements, which have to be fulfilled during the array analysis. If the result at one array is unstable, this array is not used for the analysis. This further reduces the number of events. (see lines 214-220) Nevertheless, if the noise conditions are good (especially during nighttime), we are able to determine the epicenters of very small earthquakes ($M_L < 0.5$), where it can be hard to find the onset of the P-wave at all stations. This is one of the strong advantages of the

array analysis. If we combine multiple arrays, we are able to determine the epicenter of an event without the knowledge of a velocity model.
We added this point in the revised manuscript.
Changes: lines 248-252.

R2: Line 149-151: how do you know the events are volcano-tectonic or hybrid? Have they been located and classified before? Where does that information come from? Reference?

A.: In contrast to a volcano-tectonic earthquake, a hybrid event shows a smooth transition from higher to lower frequencies. In the case of a hybrid event there is no S-phase identifiable and in the coda (for about 15 to 20 seconds) there is still more energy available in the 0-10 Hz band than before the event (and in comparison with a VT earthquake). In contrast, even for the small VT earthquakes on Fogo two phases are detectable. To make this point clearer, we replaced the example earthquake displayed in Figure 8a (formerly 7a) with an earthquake from Fogo. By this, the difference between the event types should become clearer. Additionally, we added a figure to the supplementary material which shows the spectrogram of all components of a hybrid event. In this figure the low frequency content of the coda becomes evident.
A description of such events in previous literature on volcanic seismicity is e.g. found in McNutt (2000) or Wassermann (2012). The references are given in the introduction, lines 50-52.
With our discrimination between volcano-tectonic earthquakes and hybrid events we also follow earlier studies on the seismicity of Fogo (e.g. Faria and Fonseca, 2014, references in lines 267, 313).
Changes: lines 237-238, Fig. 8, Fig. S9.

R2: Also this part (4. Results) happens abruptly, without much leading into. Has the multi-array method been applied to known events? Or is it used on traces without knowing that there is an event? Please re-write. Much of the discussion seems to have to move to results section for a better flow and a better understanding of what has been done here.

A.: The traces were inspected by eye after application of a trigger mechanism. We added this information to the results section in the revised manuscript.
As stated above, we moved the part on the error considerations of the multi-array analysis to the method section 3.
Changes: lines 145-205, 209-210.

R2: Especially the event in Figure 6 is determined by 2 arrays, why do you need the third one there? How much better becomes the location if using three arrays? How much worse is the result when using classical locations?

A.: Some of the events are indeed located using two arrays, if the third array shows e.g. unfavorable noise conditions or if the event cannot be analyzed with the third array due to an unstable result during the beamforming. In such a case, the event will be located at the intersection of the main beams (i.e. by "drawing" a line from the backazimuth for which the amplitude of the sum trace reaches its maximum).
However, the more arrays are incorporated in the analysis, the more information are included, too. For example, Figure 7 (formerly 13) shows, that the event is not located at the crossover of two main beams, but rather in between. This is the case, as the highest level of overlapping occurs in the range of the errors of the main beams. This is an advantage of the multi-array method, as the errors of the beamforming are directly taken into account during the localization of the event.

R2: In the introduction, the authors mention that the lack of S-waves makes it a good event for multi array analysis. I think it is more like the lack of S-waves makes it difficult for other location methods and that's why multi-array method can help?

A.: Yes, indeed. However, if the goal is to test the advantages of a multi-array approach it also makes sense to test it on events, which cannot be located reliably with classical localization methods.
Nevertheless, we discarded this sentence in the revised manuscript.
Changes: line 52.

R2: The description in 3.2 is confusing, please clarify, refer to the example (e.g. Figure 6?) and explain what it means to intersect the broad beam in steps of 1%...

A.: We clarified this and added an additional figure to the supplements.
Changes: lines 127-138, Fig. S3.

R2: If the velocity model of Vales et al., 2014 is used for the classical location technique, why is this not used for the other technique? There a simple generic layer model seems to be used?

A.: The determination of the epicentral distance using the S-P travel time difference is an approximation to serve as reference for the analyst. The velocity model of Vales et al. (2014) is used here to determine Moho depth, mean crustal and mantle velocities. We included this description in the revised manuscript.
Changes: line 198.

R2: Technical Points:

I may be wrong but at least one trace (4) in Figure 3a seems to be reversed in polarity. Have the traces been inspected for polarity changes? How much does the waveform complexity in this event influence the energy stacks?

A.: Trace 4 in Figure 3a is not reversed in polarity. Due to the red line overlaying the traces, it might appear like this. However, the red line is directly above the minimum of this amplitude. In Figure 3c it is better to see, that this trace shows the same polarity as the other traces. The difference between the trace 4 in Figure 3a and 3c is only a time shift, therefore the polarity does not change during this procedure.

In general, different polarities of the traces would make the beamforming impossible. It is based on the assumption, that the same phase at all traces is used for the shifting and stacking. The constructive interference of the phases leads to a reduced SNR of the sum trace. Different polarities, however, would lead to destructive interference.

We perform the array analysis manually, this means, if different polarities would occur, the analyst would recognize this. Therefore, we can assure to only perform the beamforming on the same phases. Additionally, we focus on the first arrival of the P-wave. This ensures, that the same phase is chosen at all arrays. This is important for the multi-array analysis to ensure, that the same phase is analyzed (lines 183-184).

R2: Line 166 needs a reference.

A.: This information is given in most seismology textbooks. Nevertheless, we included the information, that this only holds true for rays propagating downward from the source.
Changes: lines 224-226.

R2: Line 81: I would add local to earthquakes. For teleseismic events this is not necessarily the case.

A.: Thank you for pointing this out. We added this term in the revised manuscript.
Changes: line 81.

R2: Figures: Please add the colour bars in slowness-backazimuth plots with relevant information.

A.: We adjusted the figures accordingly.
Changes: Fig. 3, Fig. 11, Fig. S2.1, Fig. 2.2.

R2: Lines 109-111 seems to be irrelevant for the manuscript at this point? it does not fit into the flow and it knowledge that should be known.

A.: The angle of incidence is used further below to estimate the ray path of the waves of hybrid events. Therefore, it needs an introduction, which is best placed at the description of the parameters which result from the array analysis.

Changes made to figures

Formerly Fig. #	**New Fig. #**	**Changes**
1	1	--
2	2	--
3	3	Colorbar with relevant information added
4	S2.1	Colorbar with relevant information added Moved to supplementary material
5	S2.2	Colorbar with relevant information added Moved to supplementary material
6	4	Error bars corrected Figure caption changed
7	8	8a: Earthquake from Brava replaced by earthquake from Fogo Figure caption changed
8	9	Plot of the accumulated number of events adjusted
9	10	--
10	11	11a: Error bars corrected 11b:Colorbar with relevant information added
11	5	Depiction improved Figure caption changed
12	6	--
13	7	--

Multi-array analysis of volcano-seismic signals at Fogo and Brava, Cape Verde

Carola Leva[1], Georg Rümpker[1] and Ingo Wölbern[1]

[1]Institute of Geosciences, Goethe-University Frankfurt, Altenhöferallee 1, 60438 Frankfurt am Main, Germany

Correspondence to: Carola Leva (leva@geophysik.uni-frankfurt.de)

Abstract. Seismic arrays provide tools for the localization of events without clear phases or events outside of the network, where the station coverage prohibits classical localization techniques. Beamforming allows the determination of the direction (backazimuth) and the horizontal (apparent) velocity of an incoming wavefront. Here we combine multiple arrays to retrieve event epicenters from the area of intersecting beams without the need to specify a velocity model. The analysis is performed in the time domain, which allows to select a relatively narrow time window around the phase of interest while preserving frequency bandwidth. This technique is applied to earthquakes and hybrid events in the region of Fogo and Brava, two islands of the southern chain of the Cape Verde archipelago. The results show that the earthquakes mainly originate near Brava whereas the hybrid events are located on Fogo. By multiple-event beam-stacking we are able to further constrain the epicentral locations of the hybrid events in the north-western part of the collapse scar of Fogo. In previous studies, these events were attributed to shallow hydrothermal processes. However, we obtain relatively high apparent velocities at the arrays, pointing to either deeper sources or to complex ray paths. For a better understanding of possible errors of the multi-array analysis, we also compare slowness values obtained from the array analysis with those derived from earthquake locations from classical (local network) localizations. In general, the results agree well~~,~~. ~~however~~Nevertheless, there occur some systematic deviations of the array-derived backazimuth and slowness values~~, the arrays also show some aberrations~~ that can be quantified for certain event locations.

1 Introduction

Many typical volcano-seismic signals, such as long-period events or tremors, lack clear and impulsive phases. To retrieve information about the characteristics of these events, including their hypocenters, multiple small-aperture seismic antennas have been utilized in past studies at different volcanoes. For example, Almendros et al. (2001a,b) were able to resolve a detailed 3D image of the source region of long-period events at Kilauea, Hawaii, using three arrays. The same arrays were used to discriminate between different wave field components of Kilauea volcano, such as background tremor or surface waves (Almendros et al., 2002). The source of explosion quakes at Stromboli volcano, Italy, could be located using two seismic antennas (La Rocca et al., 2004). Also Etna, Italy, has been the subject to multi-array studies. For example, Saccorotti et al. (2004) deployed two arrays in 1999 to locate sources of tremor during a decreasing eruptive activity. The tremor of the 2004-2005 eruption has been the subject of the double seismic antenna study of Di Lieto et al. (2007). Almendros et al. (2007)

provided a model of the possible causes of seismicity during the seismic crisis of Teide volcano, Tenerife, in 2004 using three arrays. The sources and mechanism of vulcanian explosions of Ubinas volcano, Peru, were analyzed with two seismic antennas by Inza et al. (2014). In 2014 the VolcArray study has been performed at Piton de la Fournaise, La Réunion, with three seismic arrays, each consisting of 49 stations (Brenguier et al., 2016). By applying array techniques and ambient noise cross correlations, multipath body waves could be separated and direct and reflected surface waves were extracted (Nakata et al., 2016). The data from the same arrays have also been used by Mao et al. (2019) who monitor relative changes of the velocity in the shallow crust and by Takano et al. (2020) who are able to resolve velocity changes below the detection limit of geodetic measurements from ballistic waves. These examples represent only a small selection of multi-array studies at volcanoes, however, they are indicative of a wide range of possible applications.

In this study we use multiple seismic arrays to investigate the seismic activity of Fogo and Brava. The two islands are located in the southwest of Cape Verde (see inset Fig. 1), about 700 km west of Senegal in the Atlantic Ocean. Their volcanic origin is attributed to a mantle plume beneath the islands (Courtney and White, 1986). Fogo volcano shows frequent eruptions with intervals of about 20 years, where the last took place from November 2014 to February 2015 (González et al., 2015). This is in contrast to the other volcanoes of the Cape Verde islands, which did not experience eruptions since the settlement in 15th century. Nevertheless, there is evidence for volcanic activity beneath and around the western islands of both (northern and southern) chains of the Cape Verde. The activity occurs either beneath the islands or offshore in fields of submarine volcanic cones, including the Cadamosto Seamount southwest of Brava (Faria and Fonseca, 2014; Vales et al., 2014; Leva et al., 2020). It also involves the high seismic activity beneath and around Brava. This seismicity is characterized by a shift in location over time and frequent variations in the intensity of the seismic activity (Leva et al., 2020).

Despite the frequent volcanic eruptions, Fogo shows a rather low rate of seismicity compared to its neighbour Brava. In Fogo, we mainly find seismic events with a transition from high to low frequencies and without clear S-phases. This type of event has been described as hybrid event, combining the features of a volcano tectonic event in the signal onset and of a long-period event with respect to the coda (e.g. McNutt, 2000; Wassermann, 2012). ~~The lack of S-phases makes this type of event a good candidate for the analysis with seismic arrays.~~ For the localization of the epicenter of these events we perform a time-domain multi-array analysis. This type of analysis has the advantage of being independent of velocity models. The velocity structure is often very complex in ~~a~~ volcanic environments~~regime~~ and there is, so far, no detailed 3D-velocity model available for Fogo volcano or Brava island. The time-domain array analysis allows for the incorporation of a narrow time window while including a broad frequency band (Singh and Rümpker, 2020; Leva et al., 2020). Traces are shifted and stacked in the time domain to increase the SNR and to retrieve information about the incoming wavefront (i.e. the backazimuth and the magnitude of the horizontal slowness, which corresponds to the inverse of the apparent velocity (Rost and Thomas, 2002)). ~~This information includes the backazimuth of the ray path, pointing towards the direction of the incoming wavefront, and the magnitude of the slowness, which is defined as the inverse of the apparent velocity of the wavefront travelling across the array (Rost and Thomas, 2002).~~ Including multiple arrays allows the localization of the event in the area of the intersected beams. In our study, we operated three arrays, two on Fogo, one on Brava, and seven short-period single stations from January 2017 to January

2018. We focus on volcano-tectonic earthquakes originating in the study area around Brava and Fogo, and on hybrid events occurring on Fogo. However, due to ray bending, systematic deviations in ~~seismic arrays can exhibit systematic aberrations of~~ backazimuth and slowness values can be observed. To investigate these ~~aberrations~~ deviations at~~of~~ the three arrays of our study, we compare multi-array localizations with locations derived from standard (network-based) localization techniques (see e.g. Krüger and Weber, 1992). These standard techniques are based on the picking of P- and S-phases. For this comparison, earthquakes occurring within the network are chosen, i.e. earthquakes beneath or close to Brava or Fogo.

2 Network

From 18 January 2017 to 12 January 2018 we operated a total of 37 seismic stations on Fogo and Brava (see Fig. 1). Our network comprised three arrays each consisting of 10 stations. Two arrays were deployed on Fogo close to the villages of Achada Furna (AF) and Curral Grande (CG), the third one on Brava (BR). Another seven stations were operated as single short-period stations to complement the network – two on Brava, five on Fogo.

The design of the arrays ~~were designed~~is based on the array transfer function (in terms of frequency and the slowness components). The frequencies are chosen between 5 and 10 Hz, corresponding to mean dominant frequencies of the local events. Each array is circular and consists of a central station with two concentric rings with diameters of 700 m and 350 m, respectively. Four of the ten stations at each array are equipped with broad-band stations, the other six stations with 4.5 Hz short-period sensors (see lower right inset map in Fig. 1). As we expect events with mean frequencies between 5 and 10 Hz, the array is optimized for mean frequencies of 7.5 Hz. The array transfer function for 7.5 Hz is shown in the supplementary material (Fig. S1). It shows a single sharp maximum of energy and only minor secondary peaks. The circular shape of the array leads to a circular, symmetric peak in energy, which allows the detection of incoming wave fronts from any direction.

3 Method and data analysis

Criteria for applicability of the classical localization of local earthquakes are clear phases of the signal and a network distributed around the origin of the signal. If these criteria are not met, array techniques can help to locate the seismic event. By beamforming, the backazimuth and the ~~absolute~~ magnitude of horizontal slowness are determined. ~~from the horizontal components of slowness.~~ For this purpose, the coherent part of the signal is shifted in time and summed up (Rost and Thomas, 2002). This method is based on the assumption, that the wavefront approaching the array approximates a plane wave, which is a valid assumption if the distance between array and source is considerably larger than about ten times the wavelength of the signal (Schweitzer et al., 2012).

Performing an array analysis for local events using only one array necessitates an epicentral distance estimation. In a previous study, we determined the epicentral distance based on the S–P travel-time difference. We also assumed a simplified two-layer velocity model and a fixed event depth (for details see Leva et al., 2020). However, this approach may cause significant uncertainties in the localization due the choice of the velocity model. In the present study, to overcome this limitation, we

perform a multi-array analysis. This allows the intersection of the beams of each array, which provides the expected epicentral location of an event within the area of overlap. A main advantage of this method is its independence of a velocity model.

3.1 Beamforming

The array analysis is performed in the time domain. The time-domain analysis is equivalent to the incorporation of a wide frequency band, while the stacking window is kept narrow around the relevant phase, e.g. the first arrival of the incoming signal (Singh and Rümpker, 2020; Leva et al., 2020). Traces are first band-pass filtered within the dominant frequencies of the signal (Fig. 2). The cut-off frequencies are chosen in view of the waveform spectrogram. Following, an analysis window is chosen around the first onset of the signal. For the local events we analyze in this study this is typically in the range of one to two seconds. This is shown in Fig. 3a for an example earthquake at array AF. Later, traces will be shifted within this window in reference to the trace of the central array station. A stacking window (in red in Fig. 3a) of one or two periods length around the signal onset marks the phase, for which the beamforming is performed. All windows are chosen in reference to the central array station. The trace of the central station is kept fixed during the time-shift of the remaining traces. This time-shift is performed by a grid search with slowness values from -0.3 to 0.3 s/km and a grid size of 124×124. For each grid node traces are shifted accordingly and summed up. The resulting contour plot of the energy ~~stack~~ is shown in Fig. 3b. The slowness components s_x and s_y of the maximum energy are further used to determine slowness and backazimuth of the event. Slowness, apparent velocity, and backazimuth are estimated with $s = \sqrt{s_x^2 + s_y^2}$, $v_{app} = 1/s$, and $BAZ = (180°/\pi)$~~$90° -$~~ $\arctan(s_x/s_y)$, respectively. The traces, which are shifted according to the determined slowness of the event, and the corresponding sum trace are displayed in Fig. 3c. The analogue procedure for array BR is shown in Fig. ~~4~~S2.1a-c and for array CG in Fig. ~~5~~S2.2a-c.

The horizontal slowness (or ray parameter) is related to the angle of incidence by $\sin(i) = s \cdot v_c$, with the ~~mean crustal~~ velocity v_c of the upper layer beneath the array. Thus, the lower the slowness, the steeper the wavefront arrives at the array. For near-vertical angles of incidence, the slowness *s* becomes close to zero and the apparent velocity approaches infinity.

3.2 Multi-array analysis

After determining the energy grid of each array, the beams are intersected in the next step to obtain the earthquake ~~location~~ epicenter from the multi-array analysis. The standard deviation of the maximum energy is estimated in dependence of the chosen stacking window by randomly varying the start and end times of the stacking window 100 times by values between -0.2 s and 0.2 s. The values of ±0.2 s for the variation of the start and end times of the stacking window were chosen after performing tests with values between ±0.1 s, ±0.2 s and ±0.5 s. For the variation of ±0.1 s the standard deviation becomes very small. There is nearly no deviation from the original result, which means the resulting error is very likely underestimated and not reliable. Regarding the fact that some stacking windows are as small as 0.6s the variation of ±0.5 s proves to be too large and often leads to stacking windows far away from the signal phase of interest. Backazimuth and slowness values, thus, exhibit

deviations that are far too large. Examples of the stack of the 100 energy estimations are shown in Fig. 3d for array AF, Fig. ~~4~~S2.1d for array BR and Fig. S2.2~~5~~d for array CG. In some cases (like in Fig. ~~4~~S2.1d for array BR and in Fig. S2.2~~5~~d for array CG) the main beam broadens, pointing to a higher sensitivity of the event at the specific array to the choice of the stacking window. If the stack of the 100 energy estimations is comparable to the original energy stack (like in Fig. 3d for array AF), the choice of the stacking window has nearly no impact on the determined beam.

The standard deviation of the slowness value is used as the error of the slowness at each array. In the next step the beam is determined. The error in percent corresponding to the standard deviation of the backazimuth is estimated. This percentage is used to determine the energy values, which lie within this error range of the maximum energy. From the contour plot of energy, the minimum and maximum backazimuth values which frame these energy values are determined.~~For this, we chose the minimum and maximum backazimuth values corresponding to the standard deviation of the backazimuth.~~ The beam width is defined by ~~plotted between~~ these values, which implies that it accounts for ~~means it is not assumed as a straight line, but rather broadened, taking into account~~ possible uncertainties and may be asymmetric with respect to the maximum energy value. Additionally, in this way small sidelobes are included in the multi-array analysis. This can be seen in Fig. 4, where a small beam at array CG points to the south-southwest. The two values within which the beam is plotted are referred to as the outer range of the beam from here on. Due to possible errors and aberrations of the main beam, we do not expect that all three main beams intersect in the same point where “main beam” refers to the beam with the maximum energy. ~~We also take into account the shape of the energy plot.~~ The backazimuth range defined above is used to plot the related beam. However, a depiction of the beam energy with higher resolution would be desirable. To achieve this, we further intersect the broad beam in steps of 1% of the error estimated from the standard deviation. ~~The steps of 1% have been chosen, because in this case the beam is finely split up, while keeping the computing time in reasonable limits. Practically spoken, the broad beam is overlain by a second beam with a width of 99% of the standard deviation, then by a third beam of 98% of the standard deviation and so on. Now 100 beams overlay each other, getting smaller towards the main beam. These 100 beams need different values to allow the determination of the location with the highest probability when intersecting the beams of different arrays. The broadest beam, i.e. the beam with the width of the standard deviation, is assigned the smallest value and the narrowest beam, with a width of 1% of the standard deviation, the highest value.~~ Thus, we assign values from 1 (broadest beam) to 100 to each of the steps. This is further shown in the supplementary Fig. S3.

Now these beams are transferred to a map spanning the geological coordinates of the research area, with the array location as origin of the corresponding beam. The maximum value, which can theoretically be reached when intersecting the three beams, is used to normalize their values. After intersecting the beams, the area with the highest probability of the event location is determined. The last step is to choose a narrower section of the map ~~section~~that includes~~ing~~ the ~~coordinates of the~~ arrays and ~~of~~ the most likely epicenter determined in the previous step ~~highest probability determined in the step before. The section now has a finer grid, the highest probability is again estimated and represents the location of the event~~ (Fig. ~~6~~4).

We choose a confidence interval of 90% of the maximum value of the intersected area as error for the multi-array analysis.

43.3 Error considerations

Different factors have an influence on the uncertainty of the result of the multi-array analysis. They can be divided into two categories: uncertainties related to the parameters of the array analysis and due effects of the ray paths. Parameters in connection with the analysis are the frequency range of the data and the length of the stacking window. Effects along the ray path from the source to the array, such as heterogeneities, can result in a systematic deviation of backazimuth and horizontal slowness at ~~aberration of~~ the array.

To test for the influence of the chosen stacking window (start and end time) and the frequencies, multiple repetitions of the analysis at one array are computed with a random variation of these parameters. Results concerning the variation of the stacking window are accounted for as described in Sect. 3.2. The same analysis has been performed for varying cut-off frequencies. For earthquakes the lower frequency is randomly varied between 2 and 8 Hz, the upper frequency between 15 and 30 Hz. For hybrid events the variation was between 1 and 4 Hz and 10 to 20 Hz for the lower and upper frequencies, respectively. The analysis is done 100 times and the resulting standard deviation is again used to display the energy beam in the multi-array analysis. The results for varying cut-off frequencies show a minor influence on the backazimuth, as demonstrated in the supplementary Fig. S4. We conclude that, for a given stacking window, the variation of the frequency band can be neglected in the error determination. The selection of the stacking window has a larger contribution to possible errors and is thus included in the analysis (see Fig. 46).

Velocity heterogeneities beneath the arrays or along the ray paths can possibly lead to a systematic bias in slowness and backazimuth determination (Rost and Thomas, 2002). This ~~aberration of the arrays~~ deviation of horizontal slowness and backazimuth at the arrays can be determined by comparing backazimuth and slowness values with those derived from a different localization technique (e.g. Krüger and Weber, 1992; Schweitzer et al., 2012). With respect to local events, we decided to locate earthquakes with a classical analysis (using the HYPOCENTER code of Lienert et al., 1986) by including all single stations of our network and one station of each array. For this standard localization technique, we apply the velocity model from Vales et al. (2014). To ensure the reliability of the classical localization, only earthquakes within or very close to the network were used. This comprises only earthquakes beneath Brava, Fogo and those located between the islands. Additionally, we only used results for which the rms values and errors of the classical analysis are small (rms < 0.25 s, errors < 5 km in longitude, latitude and depth). In total, a number of 13 events fulfilled all criteria and could be used for the comparison. Figure S5 contains a map showing the locations of the classically located earthquakes including error bars. The ~~(theoretical)~~corresponding reference backazimuth and magnitude of horizontal slowness ~~values~~ of these events ~~are (~~determined using the velocity model of Vales et al. (2014)) are ~~at the different arrays and~~ compared to the respective values of the array analysis. The ~~components of the~~ resulting vectors, pointing with a blue line from the backazimuth and slowness value of the array analysis (red points) towards the respective values from the classical analysis ~~(green points)~~, are displayed in Fig. ~~11~~5. In the range of 240°-270°, array AF systematically yields backazimuths pointing too far to the south by about 7° and array CG shows backazimuth values too far to the north with a mean aberration of about 9°. The values at the array on Brava show~~s~~ a

variety of deviations due to the many directions of incoming waves. It appears, that backazimuth values in the range of 270°-360° point too far to the north. However, for the comparison with the classical localization, there are only four events within this range, prohibiting a reliable statement on systematic aberrations.

The station elevation differences of the array stations can have an impact on the result of the array analysis. Therefore, we carefully tested possible influences under the assumption of the different station elevations according to Schweitzer et al. (2012). It turned out that the station elevation differences are small enough to be neglected.

For a successful localization with multiple arrays certain requirements need to be fulfilled. For example, the stacking windows at each array should contain the same phase of the signal (Almendros et al., 2002). To ensure this, we perform the multi-array analysis on the first onset of the signal. Additionally, the occurrence of strong side lobes in the energy stack must be avoided as the occurrence of secondary peaks results in two or even more beams at one array. This may lead to event mislocations. Furthermore, the occurrence of strong side lobes generally indicates higher uncertainties in results. Regarding the intersection of the beams additional considerations must be taken into account. If beams trend almost parallel, the epicenter will be located far away with a large uncertainty in distance (see Fig. ~~12a~~6a,b). Furthermore, if two beams point from one array to another, the whole area between the arrays will be a potential source region, leading to large errors in the localization (see Fig. ~~12c~~6c,d). In these two cases the third array is of particular importance, as it will strongly narrow down the area of the likely source. If the third array does not provide any additional information in such cases the localization of the corresponding event must be discarded due to the high level of uncertainty. Also, considering that the ~~arrays~~ backazimuth and horizontal slowness show small but systematic ~~aberrations~~deviations, it is not unlikely to find a result, where the three beams do not overlap in the same area. To be able to assess the reliability of the location obtained during the analysis, information about the epicentral distance are added to the map of the intersecting beams. This can be used especially for the analysis of earthquakes: Here, S–P travel-time differences are determined for each array and plotted as circles around the array (see Fig. ~~13~~7). For this estimation we apply a two-layer velocity model with a mean crustal and a mean mantle velocity, derived from Vales et al. (2014), and a fixed event depth of 5 km (see Leva et al., 2020). This fixed event depth has been defined after estimating a mean event depth from previous studies of the region around Brava (Faria and Fonseca, 2014). However, this information about the epicentral distance is not included in the localization, as we want to retrieve the source ~~location~~ epicenter without applying a velocity model. It only serves as a reference for the analyst to evaluate whether or not the estimated source location is reasonable. Due to the lack of S-phases this estimate is not used during the analysis of hybrid events. However, here the array locations with respect to the event locations is very favourable, as the beams intersect almost perpendicular. This prevents the occurrence of parallel trending beams and beams pointing towards each other.

4 Results

The majority of the recorded events are local volcano-tectonic earthquakes mainly occurring in the area of Brava. However, we also observe hybrid events which are recorded by the stations on Fogo. Figure ~~7~~8 shows traces and spectrograms of these

two types of events. In the following we will focus on events, which were initially detected by a trigger algorithm and selected for further analysis by visual inspection.

4.1 Earthquakes

The volcano-tectonic earthquakes on average occur 8 times a day (see Fig. 98a). The rate of seismicity frequently increases, leading to phases with elevated seismic activity. 2709 earthquakes were recorded from 18 January 2017 to 12 January 2018, 112 of which could be located using multi-array techniques. The earthquakes mainly occurred around Brava (Fig. 910). The reason for the discrepancy ~~of~~ in the ~~amount~~ number of detected and ~~with the multi-array analysis~~ located earthquakes are manifold. Many smaller earthquakes are recorded with our stations only on Brava, thus precluding the multi-array analysis, as for this at least two arrays must detect the event. As described ~~further~~ in Sect. ~~4~~3.3, the multi-array analysis can only be performed for events with stable results for the backazimuth determination. If the energy grid shows e.g. strong side lobes or the choice of slightly different stacking windows for the same event leads to strongly different results, the result of this array for this particular event is discarded. Additionally, at least two arrays must show reliable and stable results, which further reduces the number of located events. The recordings of the stations on Fogo show a rather high frequency content with the main frequencies between 10 to 30 Hz (Fig. S6~~7~~a). On Brava the dominant frequencies of the same event are lower and range between 2 and 20 Hz. The corresponding spectrum is shown in the supplementary material (Fig. ~~S2b~~S6b).

The mean apparent velocities at the arrays on Fogo are in the range of 7.1 km/s for events originating close to Brava. For such a distance between event and array, the ray is first propagating downwards from the source. In a medium with lateral homogeneous velocities, the apparent velocity of this ray measured at the array is equivalent to the velocity ~~of~~ at the ray turning point. Apparent velocities <8 km/s thus point to a ray turning point within the crust (velocity model taken from Vales et al., 2014), indicating crustal depths of the earthquakes. Note that the array on Brava shows higher apparent velocities for the same earthquakes with a mean of 10.8 km/s. However, array BR is located closely to the sources, which results in a steeper angle of incidence (and smaller slowness) compared to the arrays located on Fogo.

The supplementary material contains a map with error bars of the analyzed earthquakes (Fig. S7).

4.2 Hybrid events

The hybrid events observed on Fogo (see Fig. 98b) are characterized by high frequencies (15–40 Hz) at the beginning of the signal, followed by low frequencies (1–10 Hz) and a lack of clear S-phases. The signals mainly last about 20 to 30 seconds, some last up to 1 minute, and usually reach station CV10 first, where they also show the largest amplitudes. Figure 8~~7~~b shows an example event recorded at a broad-band station of the array AF. Vertical traces of such an event are displayed in the supplementary material (Fig. S8~~3~~). The spectrograms of all components are shown in Fig. S9 and reveal the low frequency coda, where more energy occurs in the 1-10 Hz band than before the event onset. As the hybrid events were only recorded by the stations on Fogo, they were located using the arrays AF and CG. We observe 125 hybrid events, 12 of which could be located. Figure 11~~10~~a shows the resulting epicenters ~~locations~~, in or close to the collapse scar of Fogo, Chã das Caldeiras. The

events exhibit rather high apparent velocities, in average 7.8 km/s at array AF and 8.4 km/s at array CG. The mean errors of these velocities are 2.9 km/s and 2.8 km/s at array AF and CG, respectively. To determine the source location of the hybrid events, we superimpose the beams of all localizations of the hybrid events (Fig. ~~10~~11b, the area with probabilities above 80% of the maximum stacked probability is marked with a white line). We find this area in the north-western part of Chã das Caldeiras.

~~4.3 Error considerations~~

~~Different factors have an influence on the uncertainty of the result of the multi-array analysis. They can be divided into two categories: uncertainties related to the parameters of the array analysis and due effects of the ray paths. Parameters in connection with the analysis are the frequency range of the data and the length of the stacking window. Effects along the ray path from the source to the array, such as heterogeneities, can result in a systematic aberration of the array.~~

~~To test for the influence of the chosen stacking window and the frequencies, multiple repetitions of the analysis at one array are computed with a random variation of these parameters. Results concerning the variation of the stacking window are accounted for as described in Sect. 3.2. The same analysis has been performed for varying cut-off frequencies. For earthquakes the lower frequency is randomly varied between 2 and 8 Hz, the upper frequency between 15 and 30 Hz. For hybrid events the variation was between 1 and 4 Hz and 10 to 20 Hz for the lower and upper frequencies, respectively. The analysis is done 100 times and the resulting standard deviation is again used to display the energy beam in the multi-array analysis. The results for varying cut-off frequencies show a minor influence on the backazimuth, as demonstrated in the supplementary Fig. S4. We conclude that, for a given stacking window, the variation of the frequency band can be neglected in the error determination. The selection of the stacking window has a larger contribution to possible errors and is thus included in the analysis (see Fig. 6).~~

~~Velocity heterogeneities beneath the arrays or along the ray paths can possibly lead to a systematic bias in slowness and backazimuth determination (Rost and Thomas, 2002). This aberration of the arrays can be determined by comparing backazimuth and slowness values with those derived from a different localization technique (e.g. Krüger and Weber, 1992; Schweitzer et al., 2012). With respect to local events, we decided to locate earthquakes with a classical analysis (using the HYPOCENTER code of Lienert et al., 1986) by including all single stations of our network and one station of each array. For this standard localization technique, we apply the velocity model from Vales et al. (2014). To ensure the reliability of the classical localization, only earthquakes within or very close to the network were used. This comprises only earthquakes beneath Brava, Fogo and those located between the islands. Additionally, we only used results for which the rms values and errors of the classical analysis are small (rms < 0.25, errors < 5 km in longitude, latitude and depth). In total, a number of 13 events fulfilled all criteria and could be used for the comparison. The (theoretical) backazimuth and slowness values of these events are determined at the different arrays and compared to the respective values of the array analysis. The components of the resulting vectors, pointing from the backazimuth and slowness value of the array analysis (red points) towards the respective values from the classical analysis (green points), are displayed in Fig. 11. In the range of 240° 270°, array AF systematically~~

~~yields backazimuths pointing too far to the south by about 7° and array CG shows backazimuth values too far to the north with a mean aberration of about 9°. The array on Brava shows a variety of deviations due to the many directions of incoming waves. It appears, that backazimuth values in the range of 270° 360° point too far to the north. However, for the comparison with the classical localization, there are only four events within this range, prohibiting a reliable statement on systematic aberrations. For a successful localization with multiple arrays certain requirements need to be fulfilled. For example, the stacking windows at each array should contain the same phase of the signal (Almendros et al., 2002). To ensure this, we perform the multi-array analysis on the first onset of the signal. Additionally, the occurrence of strong side lobes in the energy stack must be avoided as the occurrence of secondary peaks results in two or even more beams at one array. This may lead to event mislocations. Furthermore, the occurrence of strong side lobes generally indicates higher uncertainties in results. Regarding the intersection of the beams additional considerations must be taken into account. If beams trend almost parallel, the epicentre will be located far away with a large uncertainty in distance (see Fig. 12a,b). Furthermore, if two beams point from one array to another, the whole area between the arrays will be a potential source region, leading to large errors in the localization (see Fig. 12c,d). In these two cases the third array is of particular importance, as it will strongly narrow down the area of the likely source. If the third array does not provide any additional information in such cases the localization of the corresponding event must be discarded due to the high level of uncertainty. Also, considering that the arrays show small but systematic aberrations, it is not unlikely to find a result, where the three beams do not overlap in the same area. To be able to assess the reliability of the location obtained during the analysis, information about the epicentral distance are added to the map of the intersecting beams. This can be used especially for the analysis of earthquakes: Here, S–P travel time differences are determined for each array and plotted as circles around the array (see Fig. 13). For this estimation we apply a two-layer velocity model with a mean crustal and a mean mantle velocity and a fixed event depth of 5 km (see Leva et al., 2020). This fixed event depth has been defined after estimating a mean event depth from previous studies of the region around Brava (Faria and Fonseca, 2014). However, this information about the epicentral distance is not included in the localization, as we want to retrieve the source location without applying a velocity model. It only serves as a reference for the analyst to evaluate whether or not the estimated source location is reasonable. Due to the lack of S-phases this estimate is not used during the analysis of hybrid events. However, here the array locations with respect to the event locations is very favourable, as the beams intersect almost perpendicular. This prevents the occurrence of parallel trending beams and beams pointing towards each other.~~

5 Discussion

Most earthquakes occur around and beneath Brava and the seismic activity shows several periods with increased seismicity (Fig. ~~9~~8a). This is a common observation for the seismicity around Brava (Faria and Fonseca, 2014; Vales et al., 2014; Leva et al., 2020). The earthquakes originate in the crust as derived from the apparent velocit~~y~~ies measured at the arrays. Performing the time-domain array analysis allows for the determination of the epicenter of small local earthquakes ($M_L < 0.5$), although the P-wave arrival is not clearly visible at all stations. However, their combination during the beamforming results in a clear P-phase onset of the sum trace. The application of the time-domain array analysis is favourable in such a case, as a wide

frequency band can be chosen to optimize the SNR. It is worth noting, that the frequency content of the earthquake recordings on Brava ~~show in general~~generally exhibit lower dominant frequencies (supplementary material Fig. S6~~7~~2b) than the recordings of the same events on Fogo (Fig. S6~~7~~a). This is surprising, as ~~in a volcanic regime~~ higher frequencies are typically more attenuated. On the other hand, observation of high-frequency tremor around Fogo has been described by Heleno et al. (2006). These authors report on the conservation of high frequencies in a tremor signal even at larger distances (about 15 km) from the source. In September we observe some earthquakes beneath Fogo (see Fig. 10~~9~~) which occur within the shallow crust according to the apparent velocities measured at the arrays and the S–P travel-time differences. These events are located close to the area, where deep subcrustal earthquakes have been observed in August 2016 (see Fig. S~~5~~10; Leva et al., 2019). Nevertheless, due to their large difference in depth and the long amount of time between these two occurrences, we cannot establish a link between them (as due to the transport of magma from depth into the crust).

Apart from the earthquakes in September, Fogo mainly shows volcanic seismic signals, which are best described as hybrid events (in total 125 in 2017). Their origin is located in the north-western part of the collapse scar of Fogo and on top of the Bodeira wall, which surrounds large parts of the collapse scar Chã das Caldeiras. It has been discussed in previous studies (e.g. McNutt, 2000; Wassermann, 2012) that these events are caused by a combination of source mechanisms relevant for volcano-tectonic earthquakes and long-period events. One such hypothesis is a volcano-tectonic earthquake, which triggers the oscillation of a fluid-filled cavity (McNutt, 2000). At Fogo, hybrid events have been detected before (Faria and Fonseca, 2014). They were attributed to hydrothermal processes at shallow depths (several hundred meters), due to the interaction of rainwater and hot rock. This hypothesis is based on the seasonal variation of the number of hybrid events and a water table found at 370 m depth in the Chã das Caldeiras. We observe a variation in the number of events over the year of observation and compared it with the amount of precipitation per month in 2017. The corresponding figure is shown in the supplementary material (Fig. ~~S6~~S11). We find an increase of hybrid events from February to March and from ~~June to September~~September to November. The precipitation shows a small peak in March, which might correspond to the peak of hybrid events. However, the strongest peak of precipitation occurs in August. This does not directly correlate with the maximum peak in the number of hybrid events, which occurs in November. From this, we conclude that a causal relationship between precipitation rates and the occurrence of hybrid events cannot be established.

High apparent velocities of the hybrid events indicate steep angles of incidence, possibly pointing to a deep seated source. With the multi-array analysis applied in this study, it is not possible to estimate the depth of the events, as we do not include a velocity model. However, assuming a simple velocity model (adapted from Vales et al., 2014) with increasing velocity steps of 0.1 km we derive the ray path from the angle of incidence at the array until the epicentral distance is reached. This simple model yields event depths of 5 to 14 km. Additionally we considered other velocity models, which might be better suited regarding the expected complex velocity structure. Adapting a velocity model for Etna (Almendros et al., 2000) yields event depths between 10 and 20 km. The use of the velocity model for the caldera of Tenerife (Lodge et al., 2012) yields results between 3.5 and 15 km. This shows the very large impact of the velocity model on the estimation of the angle of incidence at the array and the computed ray path. The event depths estimated from the slowness values observed at the arrays and the

different velocity models would be significantly deeper than the depths reported in previous studies. There can be several reasons for such an observation. It is possible, that the source of the events has shifted to greater depths after the eruption of Fogo in 2014. This might also explain, why there is no direct correlation between the precipitation data of 2017 and the number of hybrid events. Another possibility is that the wave field is affected by path effects caused by the complex structure of the volcanic edifice (Kedar et al., 1996). These authors suggest, that a single pulse can trigger seismic waves, which then interact with heterogeneities in the elastic, loosely consolidated surrounding layers of the volcanic edifice, leading to complex harmonic seismic signals at the receiver. Such an effect is hard to discriminate from an oscillating resonator. Finally, Harrington and Brodsky (2007) provide the explanation that hybrid events are not necessarily caused by fluid motion, but by brittle failure. Low rupture velocities and strong path effects result in the long low-frequency coda. Similar effects of low rupture velocities in unconsolidated volcanic material have also been suggested to cause the signature of long-period events, rather than fluid-driven source mechanisms (Bean et al., 2014). On Fogo, ~~this~~ brittle failure at shallow depths could be caused by gravity loadings in the collapse scar after the latest eruption. ~~From these considerations, we conclude~~In view of these previous studies and of our observations, i.e. the clear signal onset, the lack of S-phases and the smooth transition from high to low frequencies without the appearance of definite dominant frequencies, we suggest that scattering effects along the ray path may explain the ~~pattern~~ distinct appearance of the ~~observed~~ hybrid events on Fogo~~, i.e. the clear signal onset, the lack of S-phases and the smooth transition from high to low frequencies without the appearance of definite dominant frequencies~~.

A complex ray path might also affect the slowness measured at the arrays. Almendros et al. (2001a) evaluate the influence of a complex 3D velocity structure of Kilauea, Hawaii, on the apparent velocity recorded at a seismic array. The results point to a ~~partly strong~~ reduction of the slowness values in comparison to a homogenous velocity model. It is likely that the complex velocity structure of Fogo has an impact on the ray path and thus leads to slowness variations. This bias could possibly result in smaller slowness values and, thus, explain the high apparent velocities we measure. However, the assumed uncertainties of the apparent velocities are rather large and should cover this bias. In addition to these considerations, we observe strong differences in the amplitudes at the stations. The amplitudes of hybrid events at station CV10 in the collapse scar are nearly twice as large as the amplitudes of the other stations on Fogo, not located this close to the source. The second station CV14 in the collapse scar was only operational during the last three months of the study. However, for the few events detected in this period, the amplitudes at CV14 are in the range of those at CV10, but the signal arrives slightly later than at station CV10. If the events would actually occur in depths of 5 to 14 km, we would not expect such a large difference in the amplitude ratios. We thus conclude, that despite the high apparent velocities, the hybrid events should actually originate from shallower depths, as already suggested by previous authors (Faria and Fonseca, 2014). Nevertheless, a hydrothermal origin may not be necessary to explain their occurrence and their real cause remains unclear. The use of a high resolution 3D velocity model or a dedicated dense network of stations placed near the observed epicenters could contribute to a better understanding of these events, as it would allow for a more precise depth estimate.

Being independent of any velocity model and able to locate the epicenters of events without clear onset of phases or offshore, outside of the network, are strong advantages of the utilization of multiple seismic arrays. However, there are certain limitations

of the multi-array analysis. The ~~arrays~~ backazimuth and slowness determined with the arrays on Fogo and Brava show a systematic deviation, which has been estimated by a comparison with classically located events. The number of reference events (in total 13) is too small for a correction of backazimuth and slowness values during the analysis. However, some relevant conclusions can still be drawn for the utilization of the multi-array technique. At the arrays AF and CG on Fogo wavefronts arrive from a range of backazimuths of 240° to 270° (see supplementary Fig. ~~S7~~S12.1). Within this range ~~of~~the backazimuth values ~~array AF~~ show~~s~~ a mean aberration to the south of 7° at array AF and ~~CG~~ a mean aberration to the north of 9° at array CG. For the array BR on Brava observed backazimuth values cover a wide range (see supplementary Fig. ~~S7~~S12.1) and slowness values can be small for events close to the array. Figure 5~~11~~ shows larger aberrations of backazimuth and slowness for events with horizontal slowness values below 0.1 s/km. The question arises, ~~if~~whether the results of array BR should generally be discarded when they show horizontal slowness values below 0.1 s/km. However, the beams related to the arrays on Fogo can easily trend almost parallel, leading to an over-estimated epicenter distance (based on comparison with the S–P travel-time difference, see Fig. 7). Therefore, the beam of the array on Brava is essential, as it usually locates the event closer to the expected location. This is shown in Fig. 6~~12~~a,b. Generally, the errors in the events location, which result from the uncertainties of the backazimuth determination at array BR are by far smaller than the errors when using only the arrays on Fogo. The distance estimated from the S–P travel-time difference serves as verification of the epicentral distance determined by the multi-array analysis (see Fig. 7). This is especially helpful when only two arrays are available for a localization. Thus, a multi-array analysis using only two arrays is still possible, but might lead to a certain amount of earthquakes that cannot be located due to the aberration of backazimuth values. For the hybrid events on Fogo, the determination of the aberration vectors is not possible due to the lack of reference localizations. The distribution of backazimuth values of the hybrid events is displayed in the supplementary material (Fig. ~~S7~~S12.2). The backazimuth values clearly indicate a location close to or in the collapse scar of Fogo. Nevertheless, a possible aberration should not lead to large errors in the localization, because of the location of the arrays with respect to the source region.

6 Conclusion

From January 2017 to January 2018 we operated three arrays on Fogo and Brava to apply a time-domain multi-array analysis for seismic events occurring in this region. This application allows the epicentral event localization without assuming a velocity model. This is a significant advantage in ~~a~~ volcanic environments~~regime~~, where the velocity structure is difficult to constrain. Additionally, we are able to ~~locate~~ determine the epicenter of offshore earthquakes outside of the network and hybrid events without clear S-phases. Although the application of the time-domain multi-array analysis has many benefits, it is necessary to evaluate possible errors of the localization, which may result from systematic ~~aberrations of the arrays~~aberrations of backazimuth and slowness values determined at the arrays. These deviations can be caused by heterogeneities along the ray path. To determine the aberrations of backazimuth and slowness values, we compare them to those derived from a classical earthquake analysis. It turns out, that the number of reference events is too small for a reliable correction. We therefore allow for relatively large location uncertainties to cover the possible aberrations.

A large number of volcano-tectonic earthquakes are located beneath and around Brava. As reported previously (Faria and Fonseca, 2014; Vales et al., 2014; Leva et al., 2020), we observe several periods of elevated seismic activity and a frequent shift of locations around the island. Additionally, a few earthquakes occur beneath Fogo in the shallow part of the crust. Some of them occur in the shallow crust in approximately the same epicentral area as deep subcrustal earthquakes of 2016 (Leva et al., 2019). However, a conclusion concerning a possible link between these two occurrences could not be made due to the rareness of such earthquakes. However, the majority of seismic events beneath Fogo are hybrid events. As shown by a joint analysis of the events, their epicenters are close to the north western part of the Chã das Caldeiras and beneath the Bodeira wall. These events show ~~significantly~~ larger apparent velocities than the volcano-tectonic earthquakes recorded with the arrays on Fogo. Most likely, these high values result from the influence of the topography and the complex velocity structure of the volcanic edifice, leading to a possible bias in the slowness determination. Additionally, the station CV10 located in the Chã das Caldeiras shows significantly larger amplitudes than the remaining stations on Fogo. We believe that the origin of the hybrid events is not as deep as the high apparent velocities would suggest. However, the origin remains unclear due to the lack of information about the depth. The application of a precise 3D velocity model or a dedicated local network could shed further light on the depth and thus on the possible source mechanism of these events.

In addition to the volcano-tectonic earthquakes and the hybrid events, we detected isolated instances of volcanic tremor, which we have not yet analyzed in detail. This will be subject of forthcoming studies.

Data availability

The data are available for download at GEOFON (https://geofon.gfz-potsdam.de, GEOFON, 2021). Please refer to Wölbern and Rümpker (2020, https://doi.org/10.14470/4W7562667842).

Author contributions

The study and the setup of the seismic arrays were initiated and conceived by IW and GR. IW was also responsible for project administration. CL analyzed the data and prepared the figures. CL wrote the manuscript as part of her PhD under supervision of GR. The manuscript was revised by GR and IW. All authors took part in the field work.

Competing interests

The authors declare that they have no conflict of interest.

Acknowledgement

This study was financed by the Deutsche Forschungsgemeinschaft with a grant to Ingo Wölbern (grant number WO 1723/3-1). The Geophysical Instrument Pool Potsdam provided the instruments. The realisation of this study was possible due to the friendly support of Bruno Faria. Additionally, we would like to thank José Levy for his support and help in customs handling, Paulo Fernandes Teixeira and José Antonio Fernandes Dias Fonseca for supporting us during field work. For their support in

the field campaign we also thank Frederik Link, Kristina Drews, Ayoub Kaviani, Joachim Palm, Nils Rümpker, Paul Matthias, Corrado Surmanowicz and Abolfazl Komeazi. We further thank Javier Almendros and an anonymous reviewer for their comments and suggestions, which helped to improve the manuscript.

References

Almendros, J., Ibáñez, J. M., Alguacil, G., Morales, J., Del Pezzo, E., La Rocca, M., Ortiz, R., Araña, V., and Blanco, M. J.: A double seismic antenna experiment at teide Volcano: existence of local seismicity and lack of evidences of Volcanic tremor, J. Volcanol. Geoth. Res., 103, 439–462, doi:10.1016/S0377-0273(00)00236-5, 2000.

Almendros, J., Chouet, B., and Dawson, P.: Spatial extent of a hydrothermal system at Kilauea Volcano, Hawaii, determined from array analyses of shallow long-period seismicity: 1. Method, J. Geophys. Res., 106(B7), 13565–13580, doi:10.1029/2001JB000310, 2001a.

Almendros, J., Chouet, B., and Dawson, P.: Spatial extent of a hydrothermal system at Kilauea Volcano, Hawaii, determined from array analyses of shallow long-period seismicity: 2. Results, J. Geophys. Res., 106(B7), 13581–13597, doi:10.1029/2001JB000309, 2001b.

Almendros, J., Chouet, B., Dawson, P., and Huber, C.: Mapping the Sources of the Seismic Wave Field at Kilauea Volcano, Hawaii, Using Data Recorded on Multiple Seismic Antennas, Bull. Seismol. Soc. Am., 92, no. 6, 2333–2351, doi:10.1785/0120020037, 2002.

Almendros, J., Ibáñez, J. M., Carmona, E., and Zandomeneghi, D.: Array analyses of volcanic earthquakes and tremor recorded at Las Cañadas caldera (Tenerife Island, Spain) during the 2004 seismic activation of Teide volcano, J. Volcanol. Geoth. Res., 160, 285–299, doi:10.1016/j.jvolgeores.2006.10.002, 2007.

Bean, C. J., De Barros, L., Lokmer, I., Métaxian, J.-P., O' Brien, G., and Murphy, S.: Long-period seismicity in the shallow volcanic edifice formed from slow-rupture earthquakes, Nat. Geosci., 7, 71–75, doi:10.1038/ngeo2027, 2014.

Brenguier, F., Kowalski, P., Ackerley, N., Nakata, N., Boué, P., Campillo, M., Larose, E., Rambaud, S., Pequegnat, C., Lecocq, T., Roux, P., Ferrazzini, V., Villeneuve, N., Shapiro, N. M., and Chaput, J.: Toward 4D Noise-Based Seismic Probing of Volcanoes: Perspectives from a Large-N Experiment on Piton de la Fournaise Volcano, Seismol. Res. Lett., 87 (1), 15–25. doi:10.1785/0220150173, 2016.

Courtney, R. C., and White, R. S.: Anomalous heat flow and geoid across the Cape Verde Rise: evidence for dynamic support from a thermal plume in the mantle, Geophys. J. Roy. Astr. Soc., 87, 815–867, doi:10.1111/j.1365-246X.1986.tb01973.x, 1986.

Di Lieto, B., Saccorotti, G., Zuccarello, L., Rocca, M.L. and Scarpa, R.: Continuous tracking of volcanic tremor at Mount Etna, Italy. Geophys. J. Int., 169, 699–705, doi:10.1111/j.1365-246X.2007.03316.x, 2007.

Faria, B., and Fonseca, J. F. B. D.: Investigating volcanic hazard in Cape Verde Islands through geophysical monitoring: network description and first results, Nat. Hazard. Earth Sys., 14, 485–499, doi:10.5194/nhess-14-485-2014, 2014.

GEOFON: GFZ German Research Center for Geosciences, available at: https://geofon.gfz-potsdam.de, last access: 14 March 2021.

González, P. J., Bagnardi, M., Hooper, A. J., Larsen, Y., Marinkovic, P., Samsonov, S. V., and Wright, T. J.: The 2014–2015 eruption of Fogo volcano: Geodetic modeling of Sentinel-1 TOPS interferometry, Geophys. Res. Lett., 42, 9239–9246, doi:10.1002/2015GL066003, 2015.

Harrington, R. M., and Brodsky, E. E.: Volcanic hybrid earthquakes that are brittle-failure events, Geophys. Res. Lett., 34, L06308, doi:10.1029/2006GL028714, 2007.

Heleno, S., Faria, B., Bandomo, Z., and Fonseca, J.: Observations of high-frequency harmonic tremor in Fogo, Cape Verde Islands, J. Volcanol. Geoth. Res., 158, 361–379, doi:10.1016/j.jvolgeores.2006.06.018, 2006.

Inza, L. A., Métaxian, J. P., Mars, J. I., Bean, C. J., O'Brien, G. S., Macedo, O., and Zandomeneghi, D.: Analysis of dynamics of vulcanian activity of Ubinas volcano, using multicomponent seismic antennas, J. Volcanol. Geoth. Res., 270, 35–52, doi:10.1016/j.jvolgeores.2013.11.008, 2014.

Kedar, S., Sturtevant, B., and Kanamori, H.: The origin of harmonic tremor at Old Faithful geyser, Nature, 379, 708–711, doi:10.1038/379708a0, 1996.

Krüger, F., and Weber, M.: The effect of low-velocity sediments on the mislocation vectors of the GRF array, Geophys. J. Int., 108, 387–393, doi:10.1111/j.1365-246X.1992.tb00866.x, 1992.

La Rocca, M., Saccorotti, G., Del Pezzo, E., and Ibanez, J.: Probabilistic source location of explosion quakes at Stromboli volcano estimated with double array data, J. Volcanol. Geoth. Res., 131, 123–142, doi:10.1016/S0377-0273(03)00321-4, 2004.

Leva, C., Rümpker, G., Link, F., and Wölbern, I.: Mantle earthquakes beneath Fogo volcano, Cape Verde: Evidence for subcrustal fracturing induced by magmatic injection, J. Volcanol. Geoth. Res., 386, 106672, doi:10.1016/j.jvolgeores.2019.106672, 2019.

Leva, C., Rümpker, G., and Wölbern, I.: Remote monitoring of seismic swarms and the August 2016 seismic crisis of Brava, Cabo Verde, using array methods, Nat. Hazards Earth Syst. Sci., 20, 3627–3638, doi:10.5194/nhess-20-3627-2020, 2020.

Lodge, A., Nippress, S. E. J., Rietbrock, A., García-Yeguas, A., and Ibáñez, J. M.: Evidence for magmatic underplating and partial melt beneath the Canary Islands derived using teleseismic receiver functions, Phys. Earth Planet. In., 212-213, 44–54, doi:10.1016/j.pepi.2012.09.004, 2012.

Lienert, B. R., Berg, E., and Frazer, L. N.: HYPOCENTER: An earthquake location method using centered, scaled, and adaptively damped least squares, Bull. Seismol. Soc. Am., 76, 771–783, 1986.

Mao, S., Campillo, M., van der Hilst, R. D., Brenguier, F., Stehly, L., and Hillers, G.: High temporal resolution monitoring of small variations in crustal strain by dense seismic arrays, Geophys. Res. Lett., 46, 128–137, doi:10.1029/2018GL079944, 2019.

McNutt, S.R.: Volcanic Seismicity, Chapter 63 of Encyclopedia of Volcanoes, Sigurdsson, H., B. Houghton, S.R. McNutt, H. Rymer, and J. Stix (eds.), 1st Edition, Academic Press, San Diego, CA, 1015–1033, 2000.

Nakata, N., Boué, P., Brenguier, F., Roux, P., Ferrazzini, V., and Campillo, M.: Body and surface wave reconstruction from seismic noise correlations between arrays at Piton de la Fournaise volcano, Geophys. Res. Lett., 43, 1047–1054, doi:10.1002/2015GL066997, 2016.

Rost, S., and Thomas, C.: Array seismology: Methods and applications, Rev. Geophys., 40 (3), 1008, doi:10.1029/2000RG000100, 2002.

Ryan, W. B. F., Carbotte, S. M., Coplan, J. O., O'Hara, S., Melkonian, A., Arko, R., Weissel, R. A., Ferrini, V., Goodwillie, A., Nitsche, F., Bonczkowski, J., and Zemsky, R.: Global Multi–Resolution Topography synthesis, Geochem. Geophy. Geosy., 10, Q03014, doi:10.1029/2008GC002332, 2009.

Saccorotti, G., Zuccarello, L., Del Pezzo, E., Ibanez, J., and Gresta, S.: Quantitative analysis of the tremor wavefield at Etna Volcano, Italy, J. Volcanol. Geoth. Res., 136, 223–245, doi:10.1016/j.jvolgeores.2004.04.003, 2004.

Schweitzer, J., Fyen, J., Mykkeltveit, S., Gibbons, S. J., Pirli, M., Kühn, D., and Kværna, T.: Seismic Arrays, in: New Manual of Seismological Observatory Practice 2 (NMSOP-2), Bormann, P. (Ed.), Potsdam: Deutsches GeoForschungsZentrum GFZ, 1–80, doi:10.2312/GFZ.NMSOP-2_ch9, 2012.

Singh, M. and Rümpker, G.: Seismic gaps and intraplate seismicity around Rodrigues Ridge (Indian Ocean) from time domain array analysis, Solid Earth, 11, 2557–2568, doi:10.5194/se-11-2557-2020, 2020.

Takano, T., Brenguier, F., Campillo, M., Peltier, A., and Nishimura, T.: Noise-based passive ballistic wave seismic monitoring on an active volcano, Geophys. J. Int., 220, 501–507, doi: 10.1093/gji/ggz466, 2020.

Vales, D., Dias, N. A., Rio, I., Matias, L., Silveira, G., Madeira, J., Weber, M., Carrilho, F., and Haberland, C.: Intraplate seismicity across the Cape Verde swell: A contribution from a temporary seismic network, Tectonophysics, 636, 325–377, doi:10.1016/j.tecto.2014.09.014, 2014.

Wassermann, J.: Volcano Seismology, in: New Manual of Seismological Observatory Practice 2 (NMSOP–2), Bormann, P. (Ed.), Potsdam: Deutsches GeoForschungsZentrum GFZ, 1–77, doi:10.2312/GFZ.NMSOP-2_ch13, 2012.

Wölbern, I., and Rümpker, G.: FoMapS: Seismic investigation of the Fogo magmatic plumbing system, Cape Verde, using multi-array techniques, GFZ Data Services, doi:10.14470/4W7562667842, 2020.

Figures

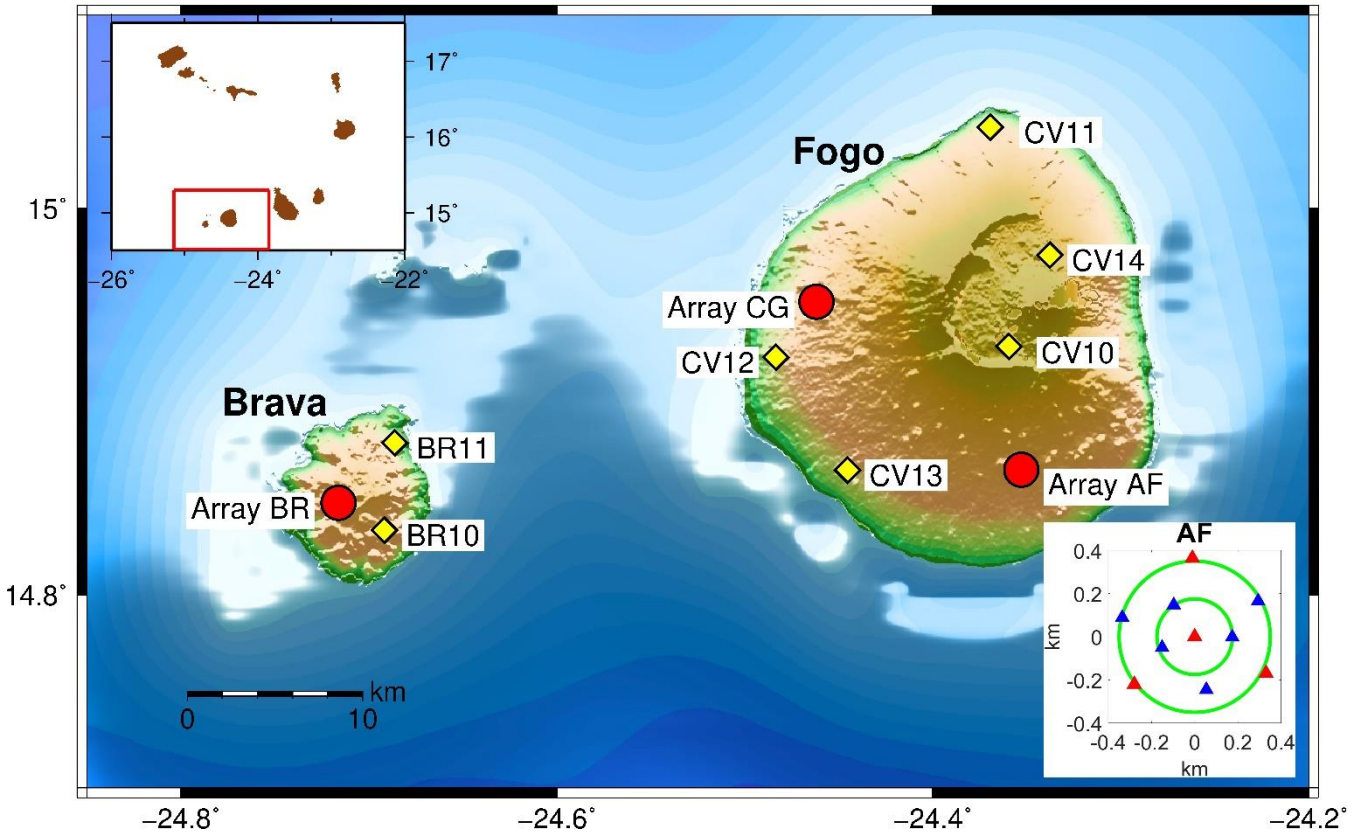

Figure 1: Station configuration on Fogo and Brava from January 2017 to January 2018. Red circles: array locations; yellow diamonds: short-period single stations. Left inset: Cape Verde, current section around Fogo and Brava marked in red. Right inset: setup of the array AF, red: broad-band stations, blue: short-period stations. The arrays BR and CG are designed in the same way. Topographic and bathymetry data are from Ryan et al. (2009).

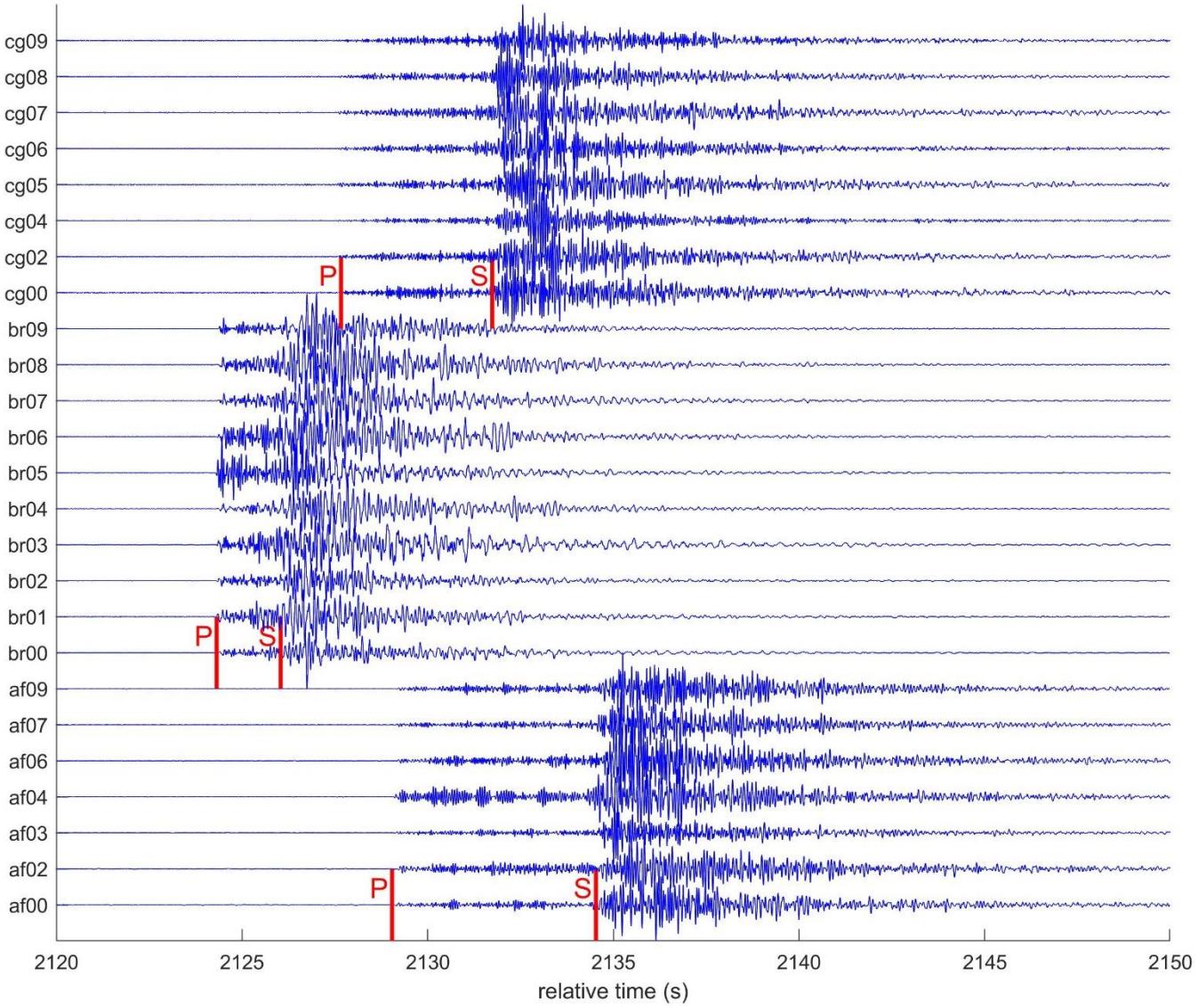

Figure 2: Z-components of the seismogram of an earthquake on 22 July 2017 (23:35 UTC) before the array analysis is performed. Traces are filtered individually according to the spectrogram of each array. Filters applied here are: 2–20 Hz at array AF, 2–24 Hz at array BR and 2–21 Hz at array CG. Red lines mark the P- and S-phases at the central array stations AF00, BR00 and CG00, respectively.

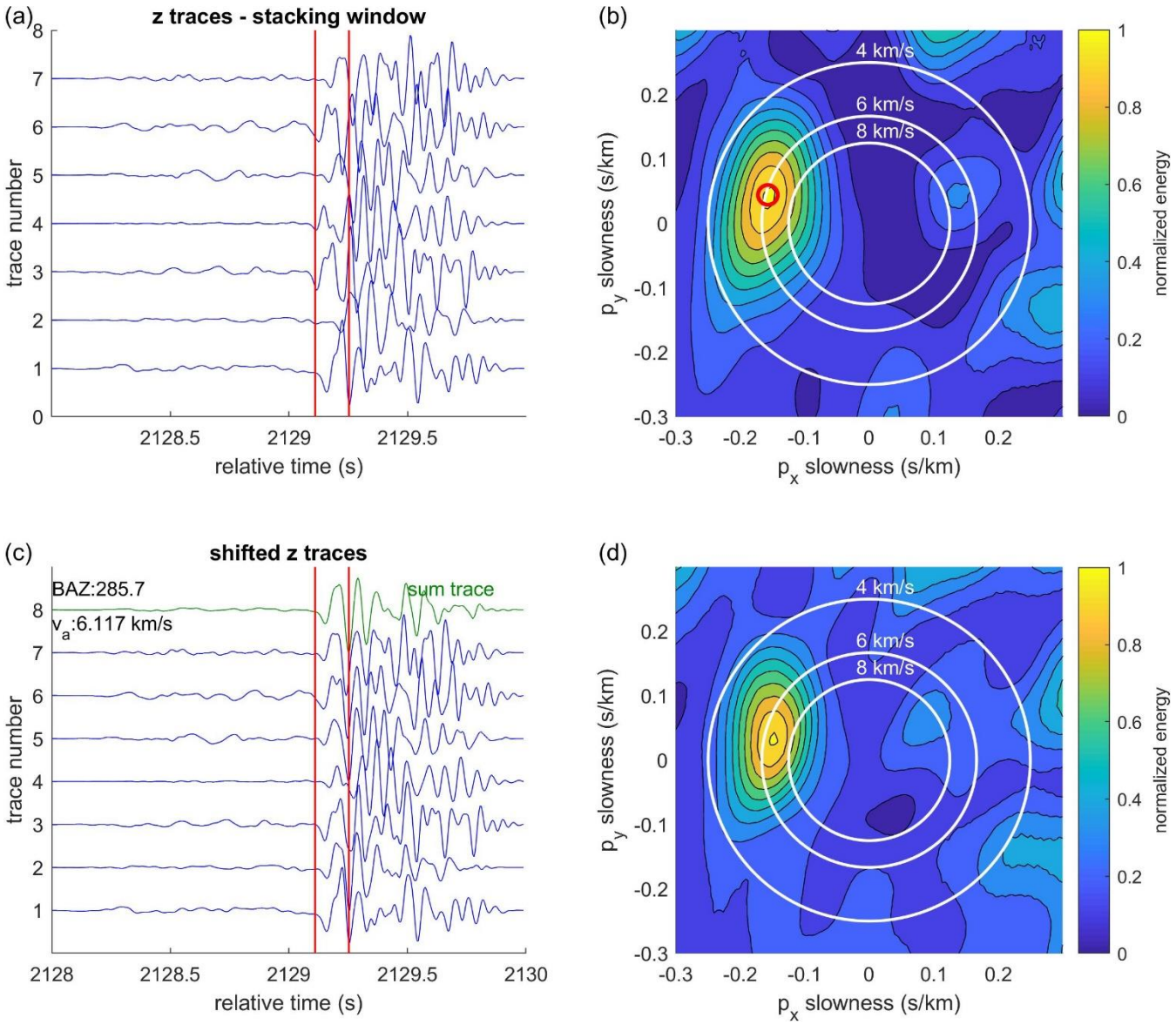

Figure 3: Time-domain array analysis of an earthquake on 22 July 2017 (23:35 UTC) at the array AF. (a) Analysis window of 2 s length with the stacking window marked in red. Traces are displayed before shifting and stacking and are filtered between 2 and 20 Hz. (b) Resulting time-domain energy stack. Red circle: maximum beam energy. (c) Time-shifted traces. The upper green trace represents the sum trace. (d) To retrieve the standard deviation of the backazimuth, the stacking window is varied 100 times by values between -0.2 and 0.2 s. The standard deviation is estimated from the 100 resulting backazimuth values. Shown here is the stack of the 100 energy plots.

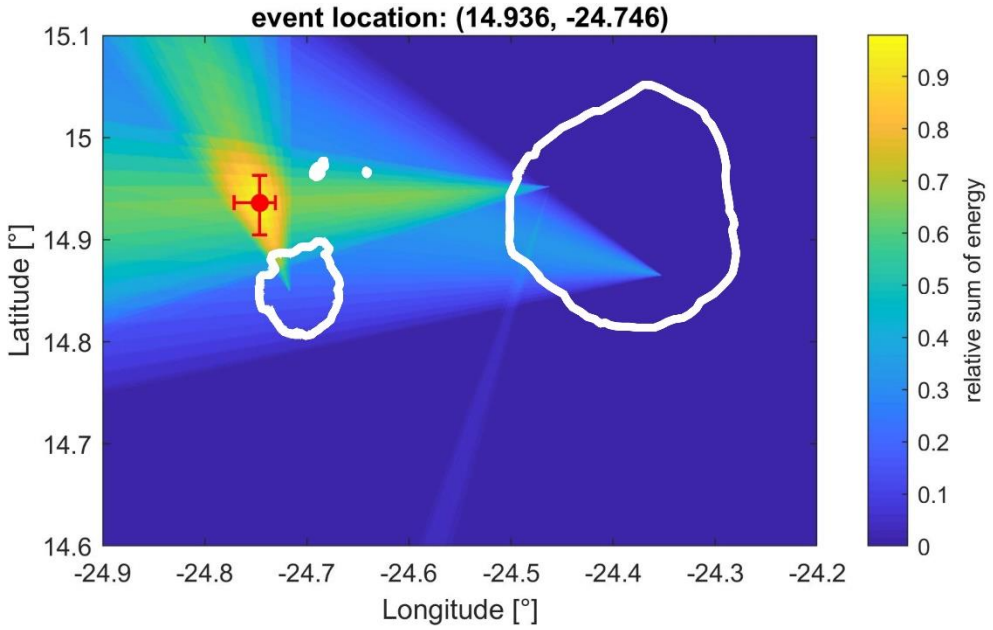

Figure 4~~6~~: ~~(a)~~ Intersection of the beams projected on a map section, including the coordinates of the arrays and the location of ~~maximum energy estimated~~the determined epicenter. The intersected beams correspond to the ~~beams determined for the~~ example earthquake on 22 July 2017 (23:35 UTC). The small beam pointing south-southwest from array CG results from a sidelobe with energy values in the range of the error corresponding to the standard deviation of the backazimuth. Red circle: event location with error bars. Topographic and bathymetry data are from Ryan et al. (2009).

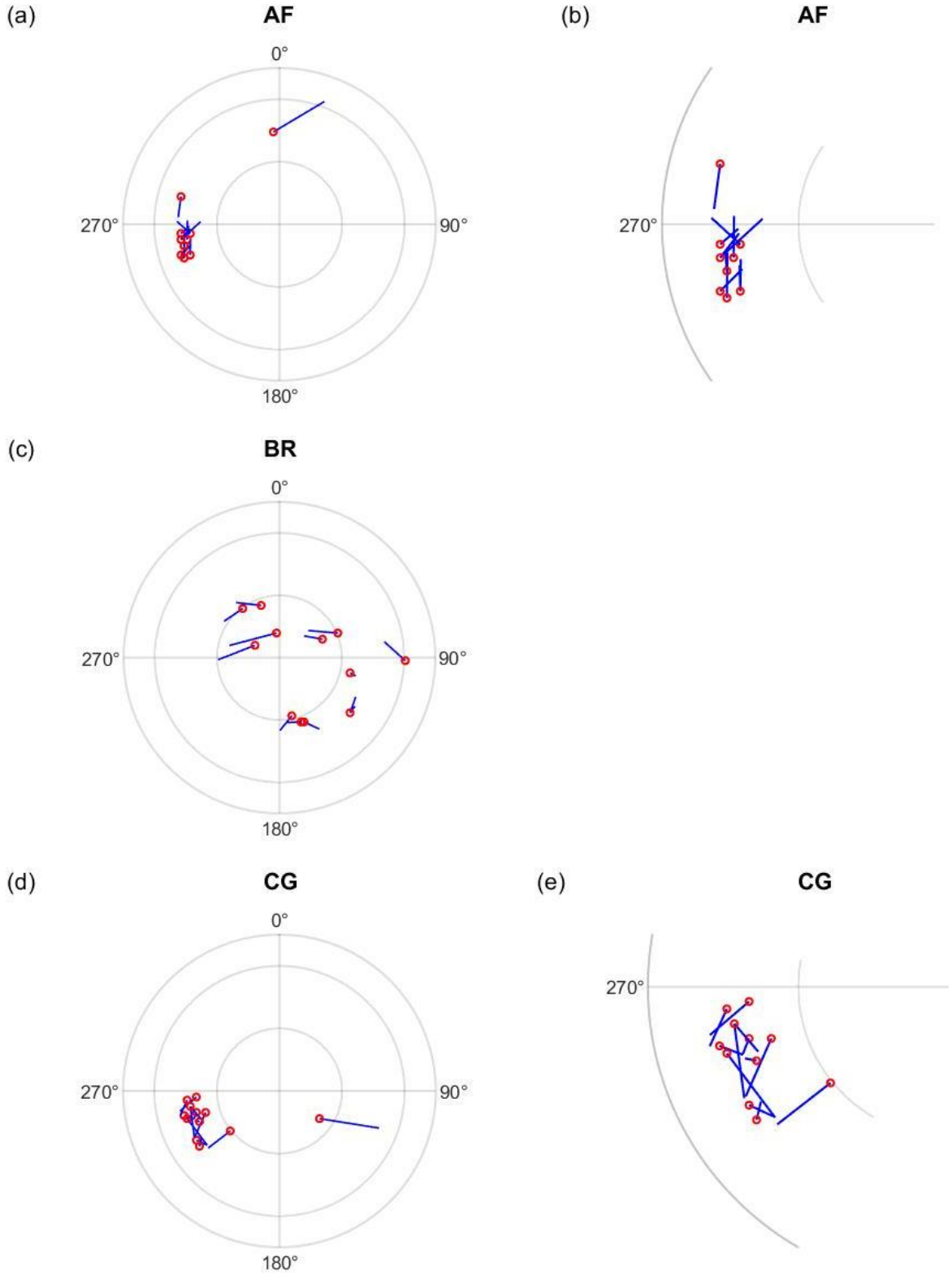
(a)
AF
0°
270°
90°
180°
(b)
AF
270°
(c)
BR
0°
270°
90°
180°
(d)
CG
0°
270°
90°
180°
(e)
CG
270°

Figure ~~11~~5: ~~Components of the aberration vectors~~Deviations of backazimuth (BAZ) and horizontal slowness. Red points: Backazimuth and horizontal slowness values of the array analysis. Blue lines point towards the corresponding reference values of the standard localization. ~~The intersections of the radius mark the slowness of 0.1 s/km, 0.2 s/km and 0.25 s/km, respectively.~~ (a) ~~Components of the BAZ aberration of~~Deviations of BAZ and horizontal slownesses, determined at array AF~~,~~. Different radii correspond to slowness values of 0.1 s/km, 0.2 s/km and 0.25 s/km, respectively. (b) ~~Components of the slowness aberration~~Deviations of BAZ in the range of 235° to 305° and horizontal slownesses at~~of~~ array AF~~,~~. The radii correspond to slowness values of 0.1 s/km and 0.2 s/km, respectively. (c) ~~Components of the BAZ aberration of~~Same as in (a) for array BR~~,~~ (d) ~~Components of the slowness aberration of array BR~~Same as in (a) for array CG~~,~~. (e) Deviations of BAZ in the range of 210° to 280° and horizontal slownesses at array CG. The radii correspond to slowness values of 0.1 s/km and 0.2 s/km, respectively.~~Components of the BAZ aberration of array CG, (f) Components of the slowness aberration of array CG. Red points: Backazimuth and slowness values of the array analysis, green points: corresponding values of the standard localization.~~

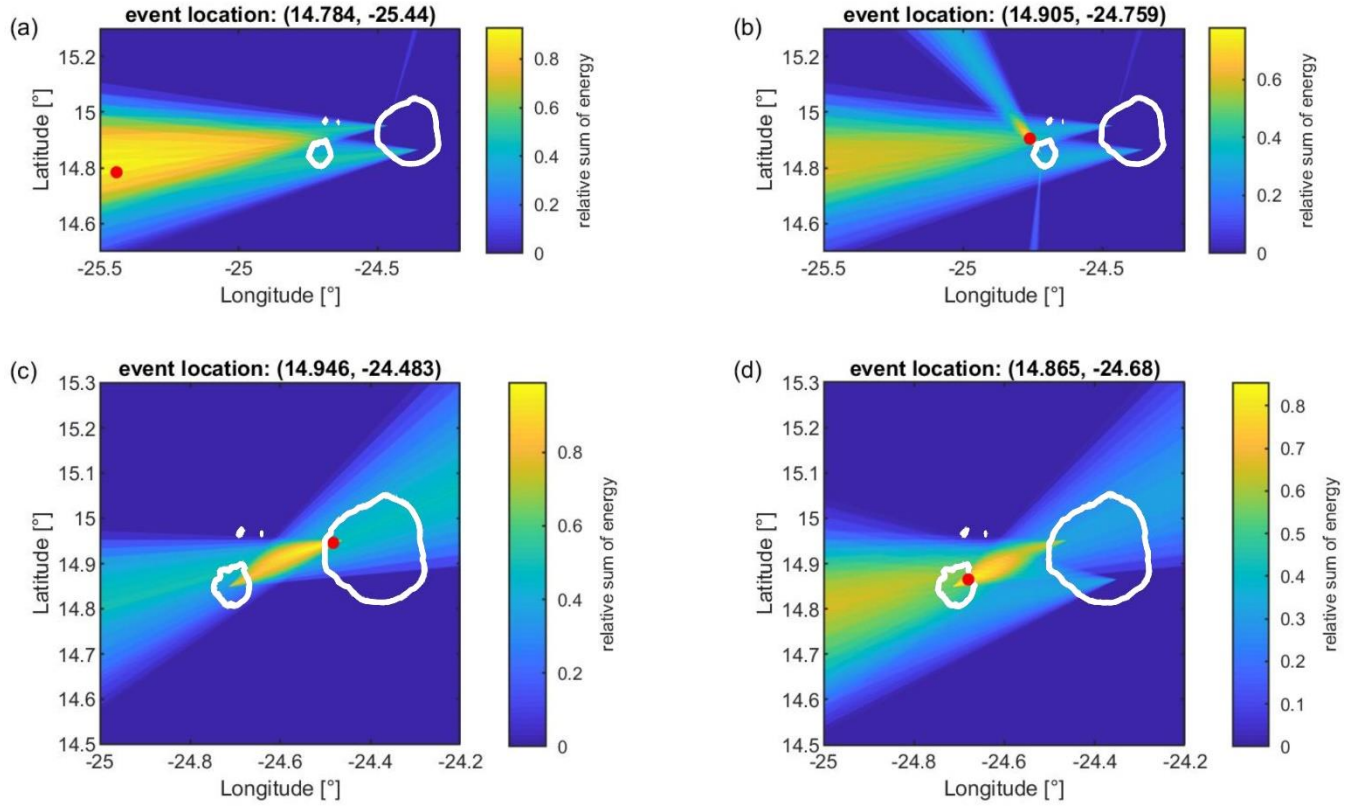

Figure ~~12~~6: Examples of ~~difficult~~ problematic localizations due to unfavourable source-receiver configurations. (a), (b) Intersection of the beams, (a) without the beam of array BR and (b) with the beam of array BR included. In the case of parallel trending beams (a) the localization of the event is distorted and the beam of the third array is needed (b). (c), (d) Intersection of the beams, (c) without the beam of array AF and (d) with the beam of array AF included. In the case of beams pointing from one array to another, (c), the ~~area~~ region of elevated ~~levels~~ energy spans ~~the~~ a large area between the two arrays. ~~and the localization of the event is distorted.~~ In this case ~~T~~the beam of the third array is needed for a proper localization (d).

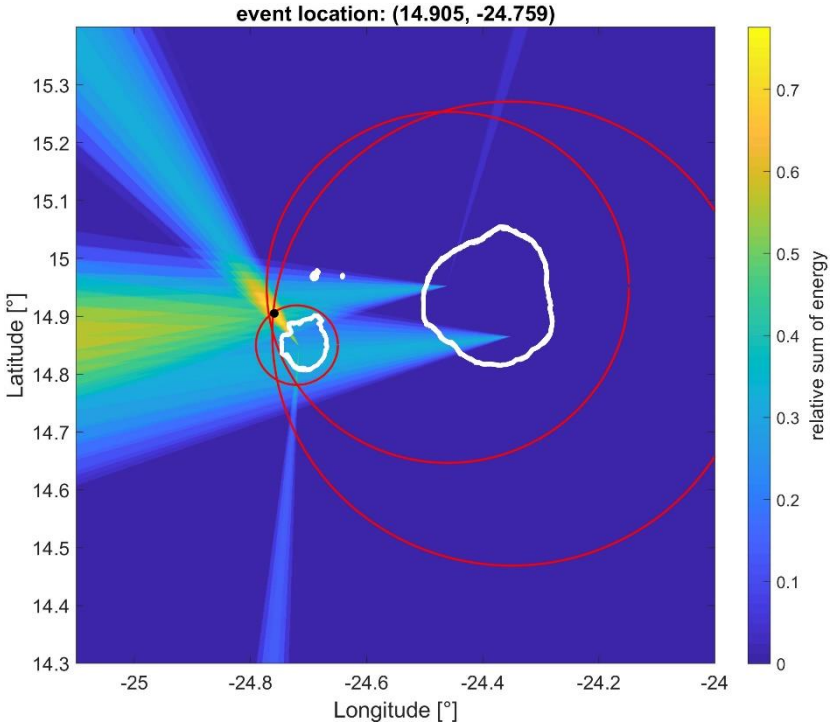

Figure 7~~13~~: Verification of the ~~result~~ event localization using additional travel-time information~~,~~. ~~b~~Black circle: location of the event derived from the intersecting beams~~;~~, red circles: epicentral distances of the event estimated from S–P travel-time differences ~~for~~ observed at the three arrays. The circles give a~~n rough~~ estimate of the expected distance of the event to the array providing a tool to better judge the reliability of the ~~outcome~~event location. Note, that this representation only serves as a support for the analyst. The final event location is only based on the multi-array analysis. ~~and is not included in the estimation of the event location.~~

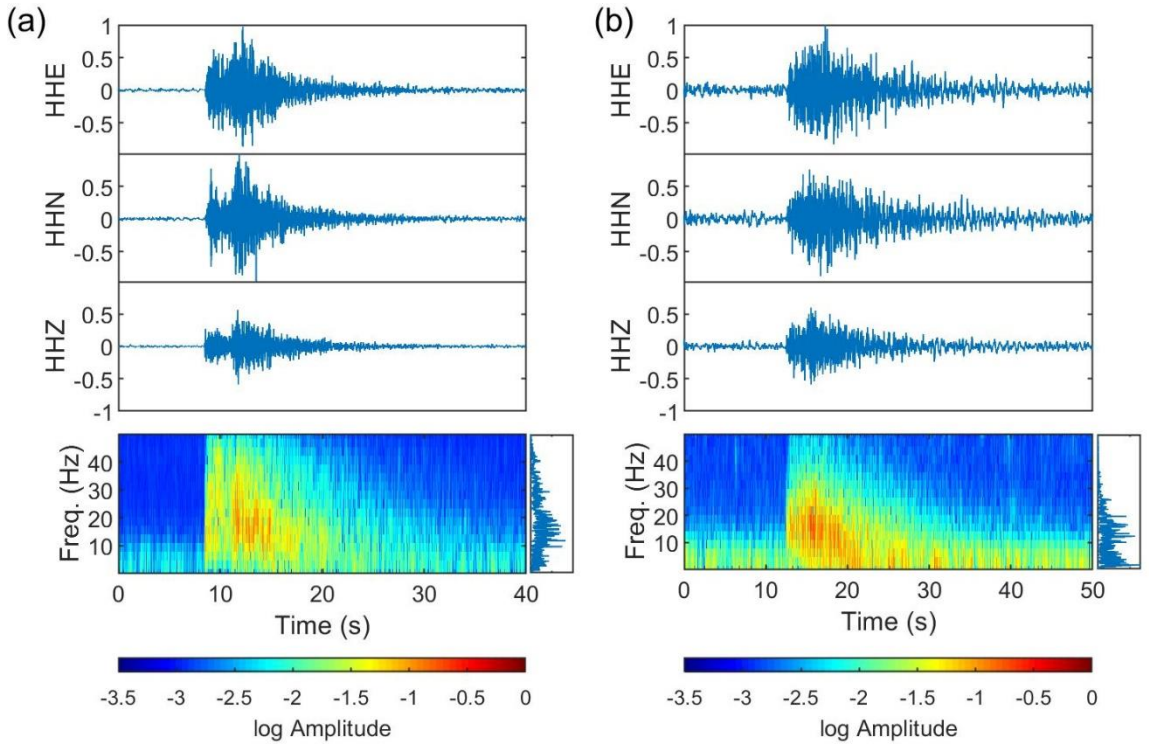

Figure 8~~7~~: Comparison of a volcano-tectonic earthquake and a hybrid event. (a) Top: Traces of an earthquake ~~occurring on~~beneath ~~Brava~~ Fogo on ~~22 Feb 2017~~18 Nov 2017 (~~16:44~~04:19 UTC) recorded at the broad-band station AF02 of array AF on Fogo. Bottom ~~left~~: spectrogram of the vertical component and overall~~, bottom right: corresponding~~ frequency content (panel on the right). (b) Traces of a hybrid event recorded on 17 Aug 2017 (02:54 UTC) at the same station. Traces are filtered between 1 and 50 Hz to remove ocean-generated noise. ~~Bottom left: spectrogram of the vertical component, bottom right: corresponding frequency content.~~ Compared to the earthquake, the hybrid event shows no clear S-phase and more energy in the 1-10 Hz band (of the coda).

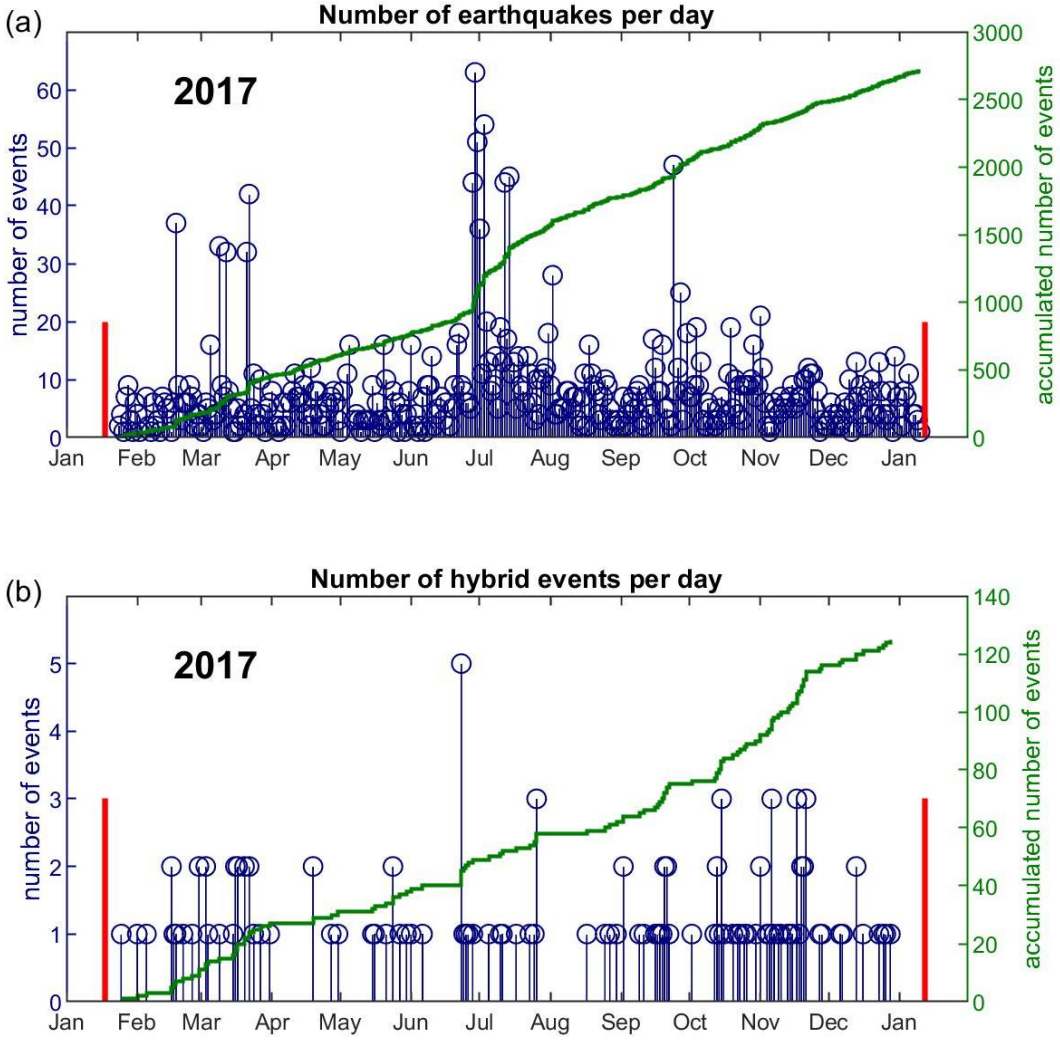

Figure 98: (a) Number of earthquakes per day. Green line: accumulated number of earthquakes. The Rrecordings range from 18 January 2017 to 12 January 2018. (b) Number of hybrid events per day. Green line: accumulated number of hybrid events during the same time period.

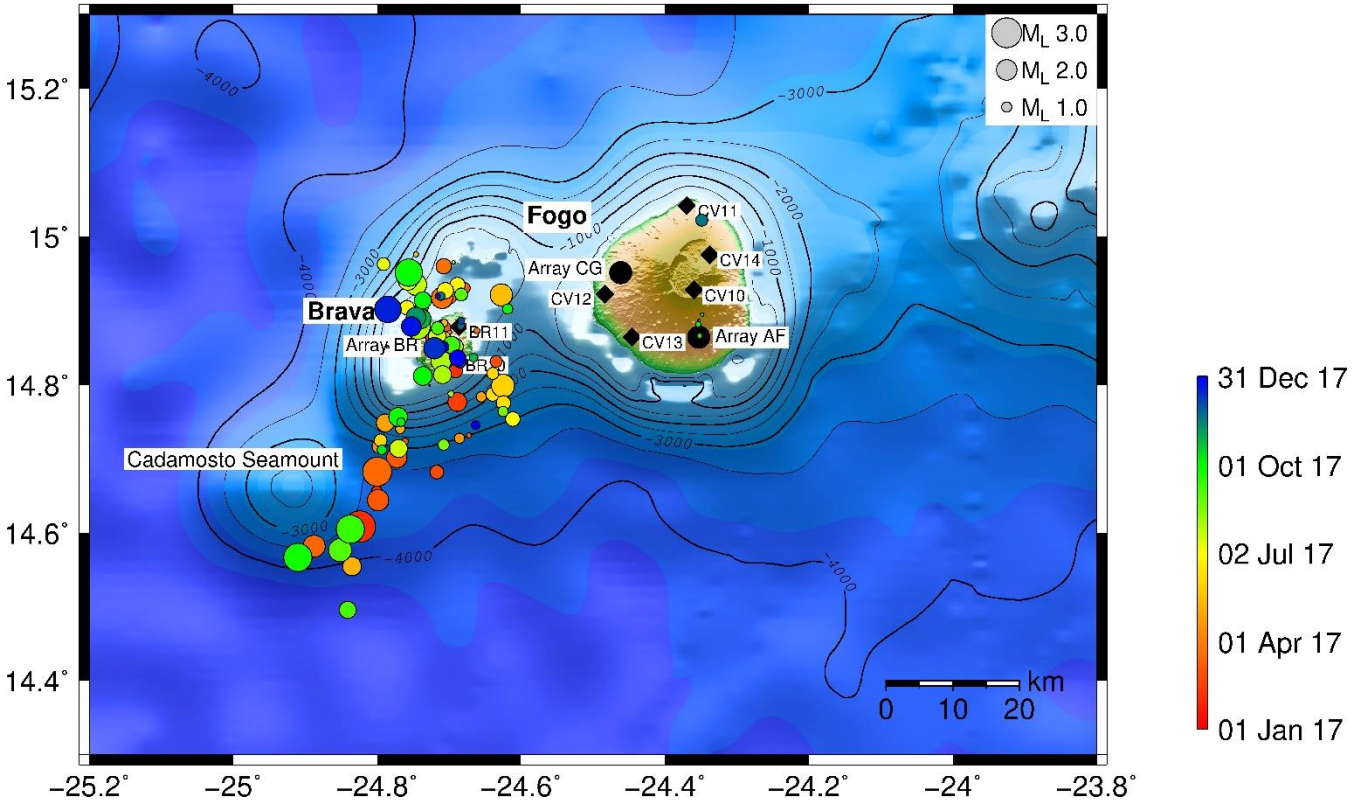

Figure 10~~9~~: Earthquake locations from 18 Jan 2017 to 12 Jan 2018. Black circles: array locations~~,~~; black diamonds: short-period single stations. Topograph~~ic~~y and bathymetry data are from Ryan et al. (2009).

615

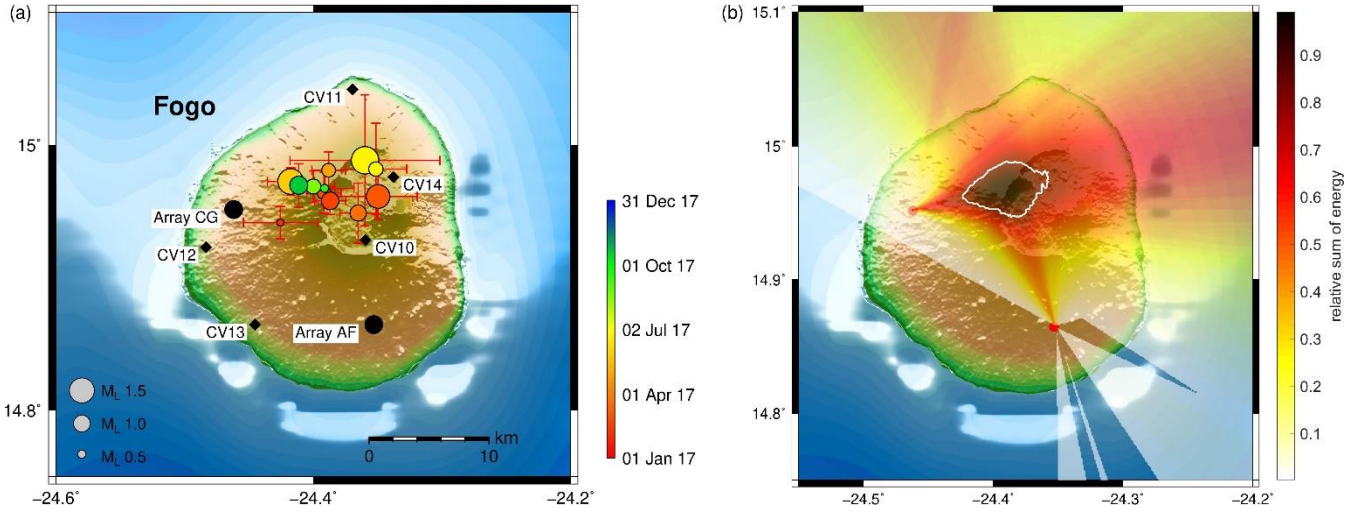

Figure ~~10~~11: (a) Locations of hybrid events detected between 18 Jan 2017 and 12 Jan 2018 and~~,~~ located with the arrays on Fogo. Black circles: array locations~~;~~, black diamonds: short-period single stations. (b) Superimposed beams of all the hybrid localizations.

~~White line: 80% of the maximum probability~~The white line corresponds to 80% of the maximum energy value and indicates a region of high probability for the occurrence of hybrid events. Topography~~ic~~ and bathymetry data are from Ryan et al. (2009).